Atmósfera 39, 321-347 (2025)
https://doi.org/10.20937/ATM.53425

Regionalization of precipitation in Guatemala in climatology and El Niño-Southern Oscillation in its Niño, Niña, and neutral phases

José Luis ARGUETA MAYORGA[1]*, Mayra Virginia CASTILLO MONTES[1], Walter Arnoldo BARDALES ESPINOZA[1] and Alfredo Salvador GÁLVEZ SINIBALDI[2]

[1] *Unidad de Modelación Matemática e Investigación, Universidad de San Carlos de Guatemala, Guatemala, 01012, Guatemala.*
[2] *Unidad de Investigación Escuela de Postgrados de la Facultad de Ingeniería, Universidad de San Carlos de Guatemala, Guatemala, 01012, Guatemala.*
*Corresponding author; email: jlargueta02@ingenieria.usac.edu.gt

Received: August 17, 2024; Accepted: February 14, 2025

RESUMEN

La regionalización de la precipitación es una herramienta fundamental para comprender los fenómenos hidrológicos, particularmente en el contexto de las fases del fenómeno El Niño-Oscilación del Sur (ENOS) (El Niño, La Niña y neutral), y su climatología en Guatemala. Este estudio introduce un marco novedoso que define límites regionales previamente difusos, revelando la naturaleza dinámica de los patrones de precipitación en el país. Los resultados demuestran cómo los límites regionales se desplazan en respuesta a las fases de ENOS, así como en condiciones de climatología y neutral. Estos hallazgos destacan la importancia de considerar la regionalización dinámica para analizar con precisión los impactos climáticos y la variabilidad de la precipitación, proporcionando una base para estrategias más efectivas de adaptación climática.

ABSTRACT

The regionalization of precipitation is a vital tool for understanding hydrological phenomena, particularly in the context of the El Niño-Southern Oscillation (ENSO) phases (El Niño, La Niña, neutral, and climatology) in Guatemala. This study introduces a novel framework that defines previously diffuse regional boundaries, revealing the dynamic nature of precipitation patterns across the country. The findings demonstrate how regional boundaries shift in response to ENSO phases, as well as under climatology and neutral conditions. These insights highlight the importance of considering dynamic regionalization to accurately analyze climatic impacts and precipitation variability, providing a foundation for more effective climate adaptation strategies.

Keywords: ENSO, cluster analysis, homogeneous precipitation, climatic boundaries.

1. Introduction

Precipitation is among the most critical hydrological variables (Gomes et al., 2018). Identifying homogeneous precipitation regions is essential for the planning, design, and management of water resource systems and infrastructure (Darand and Mansouri, 2014; Santos et al., 2015; Gomes et al., 2018; Raja and Aydin, 2019; Bhatia et al., 2020; Ilbay-Yupa et al., 2021). Furthermore, regionalization plays a key role in agricultural activities (Raziei, 2017), extreme event analysis (Bhatia et al., 2020), and hazard assessment (Zhang et al., 2016). It also enhances precipitation forecasts (Penalba and Rivera, 2016) and supports operational applications, such as seasonal measurements (Li-Juan et al., 2009). At its core, regionalization relies on combining in situ data

within homogeneous regions to better understand and predict precipitation dynamics (Parrett, 1998).

Guatemala, like many parts of the world, faces increasing challenges due to shifting climatic conditions, which have drawn the attention of scientists, policymakers, and planners globally (Shi et al., 2014). Extreme values and variability in precipitation patterns require careful analysis to ensure reliable predictions, particularly concerning the El Niño-Southern Oscillation (ENSO) phenomenon (Kolivras and Comrie, 2007). Cane and Zebiak (1985) demonstrated that this variability stems from coupled interactions between sea surface temperatures, wind stress, and ocean dynamics, which drive irregular but physically governed El Niño events, providing a basis for improving forecasts of extreme precipitation. Such analyses are critical for preventing and mitigating disasters caused by extreme precipitation events (Liu and Xu, 2016) or severe droughts (Satyanarayana and Srinivas, 2011).

Regional climate predictions have become pivotal for studying and understanding precipitation variability, especially given the unique characteristics of each geographic area. Central America has been identified as highly vulnerable to the adverse effects of climate change (de la Barreda et al., 2020), with Guatemala experiencing pronounced variability driven by ENSO phases. Bardales-Espinoza et al. (2019) found that El Niño is associated with drought conditions, while La Niña leads to increased precipitation, underscoring the significant role of ENSO in shaping regional climate fluctuations over time. These findings highlight how extreme climatic conditions drive significant fluctuations across different regions, emphasizing the need for accurate climate predictions and adaptive strategies.

ENSO plays a crucial role in modulating sea surface temperature (SST) anomalies, the displacement of these anomalies across the Pacific, as well as changes in trade winds and vertical wind shear. These factors contribute to interannual variability in the Atlantic hurricane season (Chen and Taylor, 2002; Bell and Chelliah, 2006). La Niña, the cold phase of ENSO, is associated with negative SST anomalies and increased precipitation. In contrast, El Niño, its warm phase, is linked to positive SST anomalies and decreased rainfall.

ENSO phases affect the distribution of precipitation through altered evaporation rates driven by SST anomalies and moisture transport influenced by wind flow (Maldonado et al., 2016). ENSO phases are identified based on SST anomalies in the Niño 3.4 region. An El Niño phase occurs when these anomalies exceed 0.5 ºC for more than three consecutive months, while a La Niña phase is declared when anomalies drop below –0.5 ºC for the same duration. These classifications are determined using the Oceanic Niño Index (ONI), which applies a three-month moving average of SST anomalies, updated periodically using 30-year climatological base periods.

Annual precipitation variability across Guatemala is largely driven by ENSO phases, which influence the climate system (land-ocean-atmosphere) in cycles lasting 3 to 7 years. Understanding how the El Niño, La Niña, and neutral phases affect precipitation in different regions remains a crucial research priority. With its diverse climatic regions and available databases, Guatemala is an ideal setting to study the impact of ENSO phases on precipitation distribution.

One of the main challenges in precipitation regionalization is accounting for its sensitivity to spatial and temporal variability (Srinivas, 2013). Precipitation patterns vary significantly across geographic regions (spatial variability) and fluctuate over time due to seasonal changes or extreme climate events, such as El Niño and La Niña (temporal variability). ENSO phases add another layer of complexity, as each phase induces distinct precipitation behaviors. El Niño typically leads to drought, while La Niña brings increased rainfall. Neutral phases, although less extreme, also display unique patterns. Addressing these dynamic changes requires tailored methodologies to accurately regionalize and characterize precipitation variability, providing valuable insights into climate behaviors and their implications for planning and adaptation strategies.

Delineating regions from rainfall records associated with ENSO requires robust methodologies to analyze and demarcate existing rainfall databases. Previous studies have identified two research methodology approaches linking ENSO to regionalization. The first methodology approach (Rau et al., 2017; Ilbay-Yupa et al., 2021) focuses on observing the interaction between ENSO and precipitation through the validation and characterization of identified precipitation regions. However, these studies do not segment or divide rainfall records into El Niño, La Niña,

or neutral phases; instead, they use the entire dataset and perform their analyses on a full, undifferentiated database. Furthermore, these studies correspond to different geographic contexts, spanning varying spatial and temporal scales, potentially overlooking the distinct effects of each ENSO phase on precipitation patterns and their unique regional characteristics.

The second methodology approach (Kolivras and Comrie, 2007; Miller and Goodrich, 2007) explores differentiating rainfall records by ENSO phases, dividing databases, and performing analyses based on extreme ENSO events. However, these studies lack the characterization of the identified regions and do not further investigate their specific attributes or explain the regions found.

From a geographic contextual perspective, the work of Jupin et al. (2023) identifies static regional patterns shaped by topography and ENSO phenomena, offering valuable insights into historical precipitation consistency and variability. However, the research primarily focuses on trend detection and lacks detailed exploration of short-term variability or the dynamic behavior of climatic regions. It does not address how regional boundaries shift or respond to specific climatic phases, such as El Niño, La Niña, or neutral conditions. Furthermore, the study is limited to the influence areas of the Usumacinta River, covering only a portion of Guatemala's territory, leaving out a broader analysis of regional precipitation dynamics across the country.

This research builds upon existing methodologies by aiming to regionalize and characterize precipitation patterns through three key considerations: (1) segmenting precipitation records based on ENSO phases (El Niño, La Niña, and neutral (Kolivras and Comrie, 2007; Miller and Goodrich, 2007); (2) characterizing the identified precipitation regions (Ilbay-Yupa et al., 2021; Rau et al., 2017) using variables that support informed decision-making and provide a robust foundation for future studies; and (3) addressing the sensitivity of precipitation patterns to spatial and temporal variability across the territory of Guatemala. This approach acknowledges the significant variation in precipitation across space and time, emphasizing the complexity inherent in the regionalization process.

K-means clustering is an essential tool for this study because it efficiently identifies homogeneous precipitation regions, allowing for a deeper understanding of rainfall patterns across Guatemala. Its ability to handle large datasets with quantitative variables, such as latitude, longitude, elevation, and precipitation, makes it ideal for regionalization. This method ensures clusters are representative of distinct climatic behaviors, facilitating the analysis of spatial and temporal variability. This approach aligns with the findings of Al-Qadami and Abdulla (2019), who demonstrated the effectiveness of K-means clustering in optimizing data use and delineating precipitation regions in areas with limited information. By leveraging this methodology, this research addresses Guatemala's complex precipitation variability under different ENSO phases and climatology, providing clear, interpretable results that support decision-making in water resource management, agricultural planning, and disaster mitigation.

This study aims to assess and characterize the regionalization of rainfall patterns in Guatemala from 1981 to 2020, focusing on understanding the influence of ENSO phases (El Niño, La Niña, and neutral) and climatology.

2. Data and methodology

2.1 Study area

Guatemala is located between 13º-18º N, and 88º-92º W, bordered to the west and north by Mexico, to the east by Belize, the Caribbean Sea, Honduras, and El Salvador, and to the south by the Pacific Ocean. The database was divided temporally by classifying the climatic scenarios of El Niño, La Niña, neutral, and ENSO's climatology, which allows dividing and fragmenting the database based on the years in which each of the phases occurred.

2.2 Database

A consolidated monthly rainfall database was developed using data from 159 stations, including 60 from the National Institute of Seismology, Vulcanology, Meteorology, and Hydrology (INSIVUMEH), 39 from the National Electrification Institute, 30 from the Private Climate Change Institute (ICC), four from the Municipal Water Company (EMPAGUA), and 26 virtual stations from CHIRPS (Fig. 1). The dataset spans from 1981 to 2020. To address gaps in the time series, missing data were corrected using

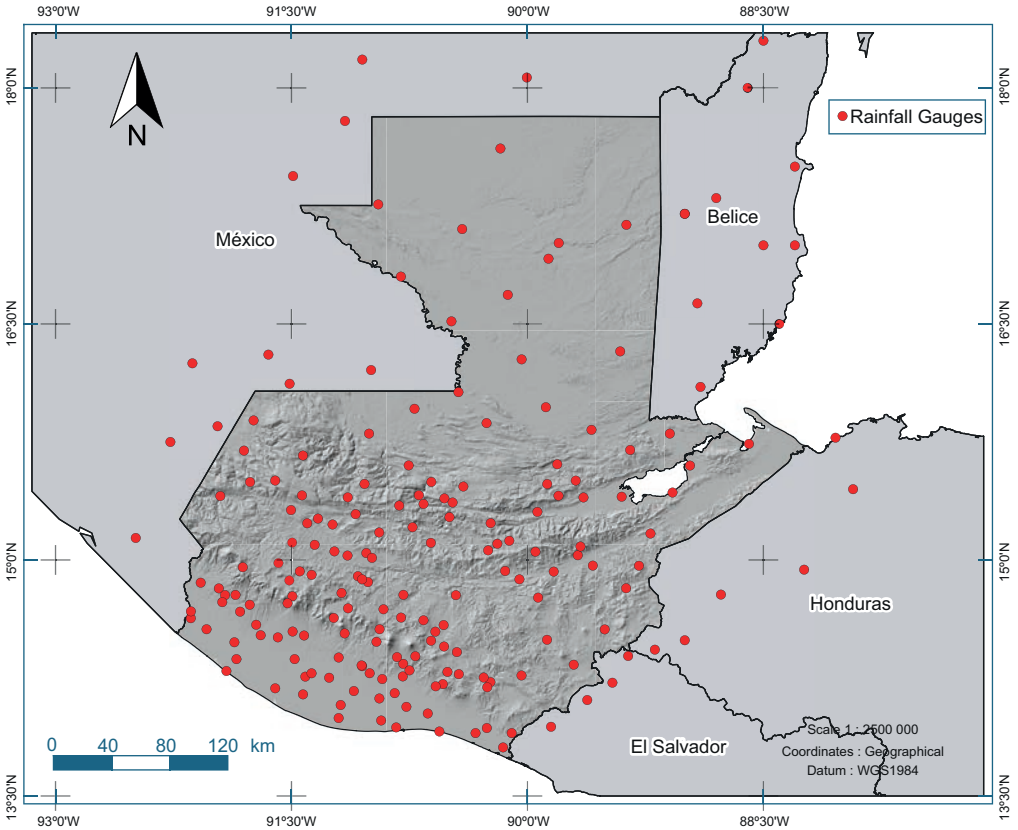

Fig. 1. Location of rainfall gauges used for conducting climate regionalization analysis.

a multiplicative bias adjustment based on CHIRPS (Funk et al., 2015). Monthly and annual averages were subsequently calculated for each station. This unified database, integrating diverse sources and time periods, provides a critical foundation for rigorous cross-study comparisons (Penalba and Rivera, 2016). Moreover, selecting appropriate data is a vital step prior to conducting regional or climatic analyses, as it can significantly impact the results and conclusions (Li-Juan et al., 2009). The variability in data sources, along with spatial and temporal scales, demands careful consideration for accurate climate predictions.

The database is fundamental for comparing various applied methodologies, as the diversity of data can lead to contrasts in the results obtained by different studies (Penalba and Rivera, 2016). This approach is critical for further exploration of databases and their derived outcomes. Additionally, the careful selection of data is indispensable before conducting regionalization or climate classification, as it may require considerations of spatial and temporal scales to ensure accurate climate predictions (Li-Juan et al., 2009).

2.3 El Niño Southern Oscillation phases

The acronym ENSO describes the natural two-way interaction between the ocean (El Niño) and the atmosphere (Southern Oscillation) in the tropical Pacific region (Hilario et al., 2009). El Niño is characterized by warm SST anomalies in the central and eastern equatorial Pacific. The Southern Oscillation (SO) is a variation in atmospheric pressure between the central/eastern Pacific and the western Pacific. These two phases are coupled into a single ocean-atmosphere system. In addition, precipitation in various regions is often correlated with ENSO using the Southern Oscillation Index (SOI) and Niño 3.4 indices (Kolivras and Comrie, 2007).

ENSO is monitored using four key Niño regions in the tropical Pacific: Niño 4, Niño 3.4, Niño 3, and Niño 1+2. These regions track variations in SST, which influence ENSO phases. Niño 3.4, located in

the central Pacific, is the primary index for defining ENSO phases due to its balanced representation of SST variability. Niño 4 monitors the western Pacific, Niño 3 focuses on SST changes in the eastern Pacific, and Niño 1+2, near South America, detects early ENSO signals.

Extreme weather events, such as those driven by ENSO, disrupt typical climatic patterns. For example, El Niño, characterized by periodic Pacific warming every 2 to 7 years, significantly alters regional precipitation patterns (Maldonado, 2016).

Additionally, variability in surface winds, particularly trade winds, appears to be related to ENSO phases. During an El Niño event in the Northern Hemisphere summer, trade winds tend to intensify, while the opposite occurs during La Niña. These patterns are evident in phases such as the Chocó Jet and the Caribbean Low-Level Jet (Poveda and Mesa, 2000; Wang, 2007; Amador, 2008).

In this research, the analysis of precipitation patterns is categorized based on ENSO phases defined by SST anomalies in the Niño 3.4 region. El Niño analysis refers to periods when SST anomalies exceed +0.5 ºC, while La Niña analysis corresponds to periods with SST anomalies below –0.5 ºC. Neutral analysis is conducted for periods where SST anomalies fall between –0.5 and +0.5 ºC. Additionally, when referring to the climatology, the analysis includes the entire dataset, encompassing all information periods regardless of the ENSO phase. This classification allows for a comprehensive understanding of precipitation variability across different ENSO conditions and climatology.

2.4 Methodology

The methodology (Fig. 2) involves consolidating precipitation data from multiple sources, including meteorological stations (INSIVUMEH, ICC, INDE, EMPAGUA) and satellite-based CHIRPS data, into a unified and comprehensive database. In cases of missing or incomplete data, adjustment parameters derived from CHIRPS were applied to ensure a complete and homogenized time series.

To address gaps and inconsistencies in the time series, missing data were corrected using a multiplicative bias adjustment based on CHIRPS, a widely recognized and validated dataset for precipitation data. This method adjusts for systematic biases by scaling observed data to align with the CHIRPS dataset, ensuring continuity and consistency across stations. The approach not only fills gaps but also harmonizes data from different institutions and methodologies, mitigating potential disparities.

Selecting appropriate and reliable data sources is a vital prerequisite for conducting regional or climatic analyses, as the quality and completeness of the data significantly influence the robustness of results and conclusions (Li-Juan et al., 2009). The source diversity of the dataset reflects varying spatial and temporal resolutions, presenting both opportunities and challenges. While this enhances its comprehensiveness, it requires careful consideration of the variability to ensure accurate climate modeling and predictions. For instance, virtual stations from CHIRPS complement physical station data by filling spatial gaps, but their integration requires validation to maintain data fidelity.

The dataset was then categorized based on the years identified by the National Oceanic and Atmospheric Administration (NOAA) as corresponding to neutral, El Niño, or La Niña ENSO conditions, as well as climatology, which encompasses the entire dataset. For each ENSO phase and the climatology, the K-means clustering algorithm was employed to perform regionalization, incorporating temporal categorization. ANOVA was used to compare regions and assess statistically significant differences in the precipitation variable across them.

Additionally, the analysis considered different time scales, including monthly, seasonal, and annual statistics, while integrating geographic and elevation information. It was significant to characterize and analyze each phase for each region to understand how precipitation patterns varied based on latitude, altitude, area, minimum and maximum precipitation, mean precipitation, length, distance to the Pacific Ocean, distance to the Atlantic Ocean, and coefficient of variation (CV). Ultimately, regions were defined for each ENSO phase, and their unique characteristics were identified, providing valuable insights into spatial and temporal precipitation variability essential for climate studies and predictions.

While characterizing the regions, a methodology (Fig. 2) was developed to identify and understand each region as a product of the regionalization process. The cokriging method was employed to achieve

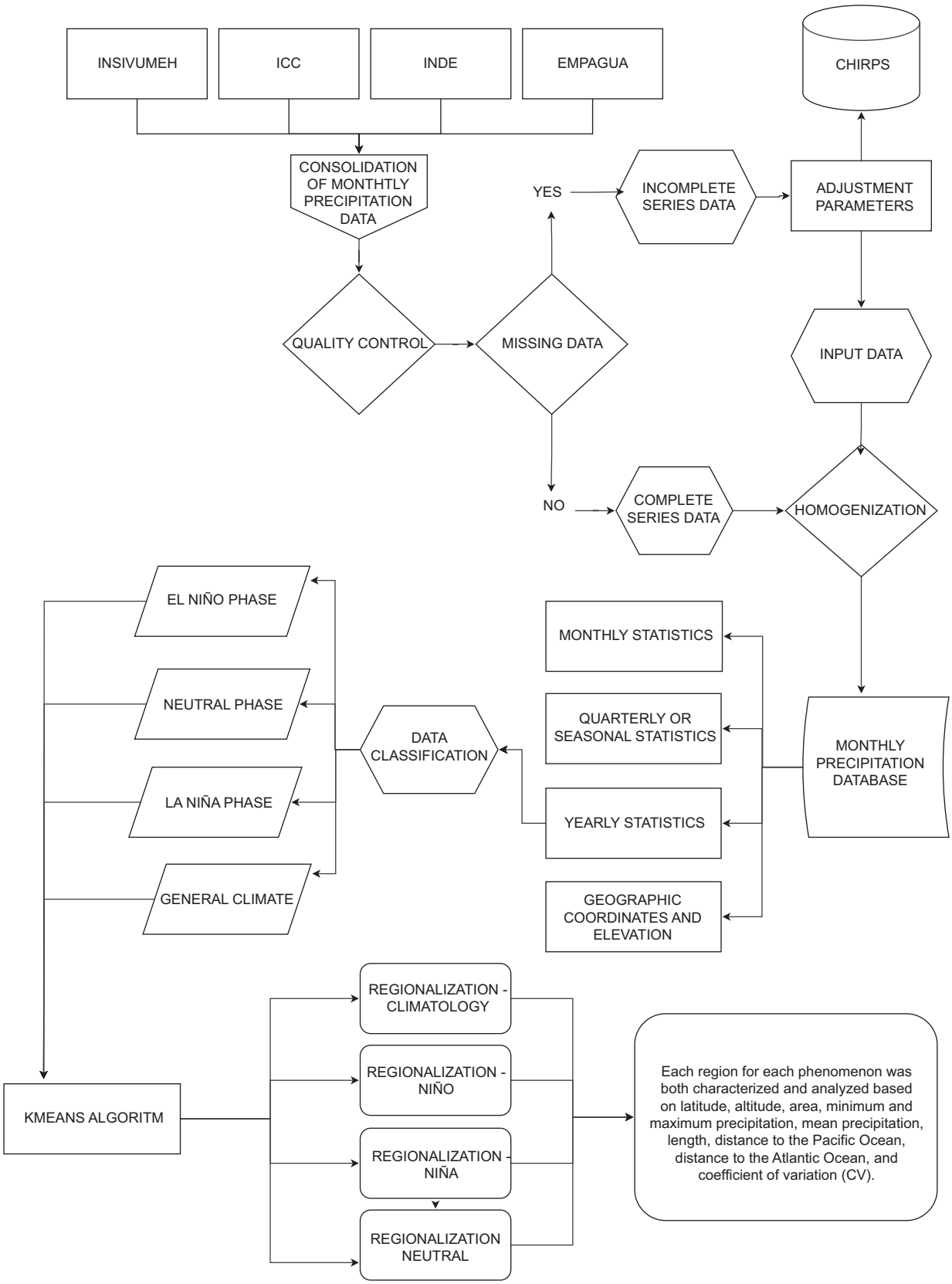

Fig. 2. Methodology applied in the process of regionalization of precipitation in different climatic phases and climatology.

an accurate interpolation of precipitation within the defined regions. This technique allowed for a detailed and reliable spatial representation of the annual precipitation variable. Additionally, it was essential to overlay the regional boundaries onto the interpolated area to ensure that the spatial patterns were accurately captured within each region.

Table I presents the data classification according to the ENSO phases. This division is essential as it forms the basis for studying climatic precipitation regions in relation to the presence or absence of the ENSO phenomenon and its impact on precipitation across the country's territory. By categorizing the data into neutral, El Niño, and La Niña conditions, rainfall scenarios associated with each phase can be compared. Additionally, the analysis includes the overall average for the entire study period, providing a baseline that does not account for the influence of specific climatic phenomena, enabling a broader understanding of precipitation variability.

2.5 K-means classification method

Cluster analysis has become increasingly significant in hydrological studies as a valuable strategy for optimizing available datasets, particularly in areas with limited information. Precipitation events are known for their considerable variability and complex distribution patterns across space and time (Al-Qadamy and Abdulla, 2019).

The K-means clustering method is widely employed for grouping individual observations into homogeneous clusters (Meddi et al., 2013; Ilbay et al., 2019). This method is an iterative process that converges by selecting representatives (centroids) for each cluster, effectively organizing data based on dominant quantitative variables (Meddi et al., 2013). One of its key advantages is its ability to form clusters based on centroid characteristics, ensuring that each cluster is both representative and meaningful (Rau et al., 2017).

For this research, the K-means algorithm was applied using variables such as longitude, latitude, elevation, monthly precipitation, annual precipitation, and the duration of the rainy season. This approach allowed for a structured classification of precipitation patterns while accounting for spatial and temporal variability.

2.6 Validation

The validation metric used was the Silhouette coefficient, which is important for defining partition groups, as it allows the assessment of the statistical significance of each identified group (Rousseeuw, 1987; Rau et al., 2017). To calculate the silhouettes, the assignment of the data through the K-means method and the collection of proximities between objects must be considered (Rousseeuw, 1987). The Silhouette coefficient calculates, for each point, a width that reflects its membership in a specific group. The average of these widths is used to assess the internal coherence of the clusters.

$$SI_k = \frac{1}{n}\sum_{i=1}^{n}\frac{(b_i - a_i)}{max(a_i, b_i)} \quad (1)$$

where n is the total number of clusters, a_i is the average distance between point i and the rest of the points in the cluster, and b_i is the minimum of the average dissimilarities between i and points in other clusters. Finally, the partition with the highest SI is taken as optimal.

2.7 Classification of regions

To demonstrate how the optimal number of clusters was selected for the different climatic phases of analysis, the result of cluster optimization for the climatology class (which includes all the precipitation

Table I. Yearly classification of ENSO conditions: El Niño, La Niña, and neutral.

El Niño	La Niña	Neutral
1982, 1983, 1987, 1991, 1992, 1997, 1998, 2002, 2004, 2009, 2015, 2019	1980, 1981, 1984, 1986, 1989, 1990, 1993, 1994, 1996, 2001, 2003, 2005, 2006, 2012, 2013, 2014, 2017	1985, 1988, 1995, 1999, 2000, 2007, 2008, 2010, 2011, 2016, 2018, 2020

Source: own elaboration from NOAA data.

periods analyzed) is presented below. The cluster plot (Fig. 3a) reveals distinct groupings of data points, with clear boundaries for most clusters, though some overlapping areas are visible. These overlapping areas can be considered transition regions, reflecting the dynamic nature of climatic boundaries. The axes Dim1 and Dim2 capture 82.6% of the data's variability, providing a robust 2D representation of the clusters and illustrating meaningful separations while retaining much of the data's structure.

The optimal number of clusters was identified using the Elbow method (Fig. 3b) and the Silhouette method (Fig. 3c). The former suggests that three clusters may be optimal, as the total within sum of squares (TWSS) significantly decreases up to k = 3, after which the reduction slows, forming an "elbow". In contrast, the Silhouette method indicates k = 2 as the optimal number of clusters, with the highest average silhouette width of approximately 0.4, reflecting the best separation and cohesion. The results highlight a

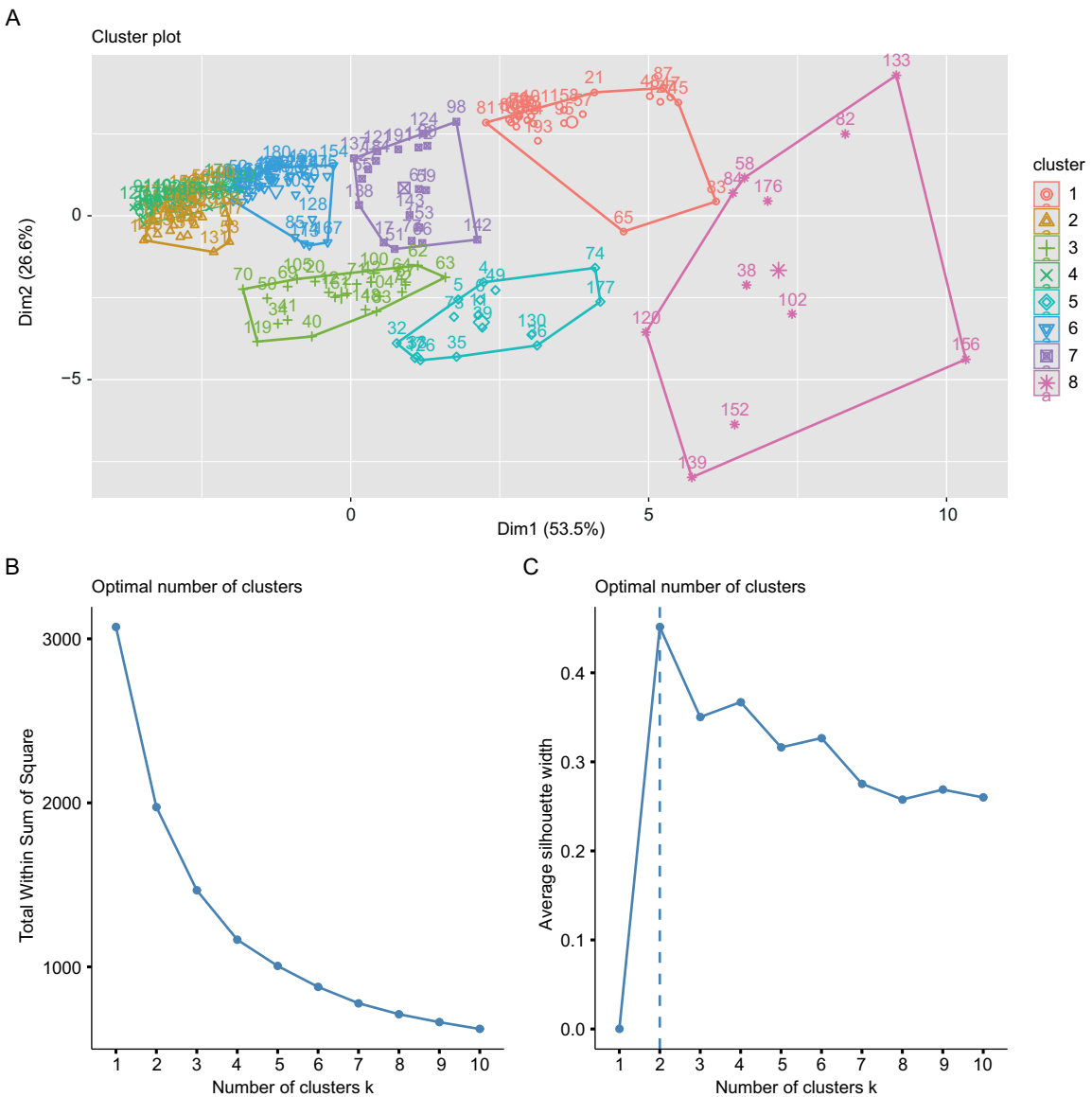

Fig. 3. (a) Biplot for eight clusters; (b) optimization of the number of clusters by the total sum of squares method; (c) optimization of the number of clusters.

trade-off between fewer, broader clusters (k = 2) and more detailed sub-groupings (k = 3). These findings emphasize the need to balance statistical optimization with practical interpretability, particularly when analyzing overlapping or transitional climatic regions, as seen in the climatology class.

The analysis of the Silhouette coefficients presented in Table II reveals that the clustering results are moderately defined, with values ranging from 0.29 for the neutral phase to 0.39 for the El Niño phase, and intermediate values for La Niña (0.36) and climatology (0.32). Positive Silhouette values indicate that the clusters are reasonably cohesive and distinct, as most data points are closer to their assigned cluster than to others; however, the relatively low values suggest some overlap or ambiguity in cluster boundaries.

Table II. Cluster summary and Silhouette coefficient.

Phase	Cluster optimization	Silhouette width
El Niño	4	0.39
La Niña	4	0.36
Neutral	6	0.29
Climatology	8	0.32

The mean Silhouette analysis suggests that two clusters would yield the highest coefficient; however, when selecting seven, eight, or nine clusters, a mean silhouette of 0.32 is achieved, reflecting a trade-off between cluster detail and quality. For the specific climatic phases, the optimal number of clusters was determined to be four for both El Niño and La Niña, six for the neutral phase, and eight for the climatology, capturing the variability and complexity inherent in precipitation patterns. The Silhouette coefficient provides a valuable metric for evaluating the effectiveness of the identified clusters, offering insight into the optimization and relevance of the regionalization process for each climatic phase.

Figure 4 displays silhouette plots for clustering results across three climatic phases: neutral (Fig. 4a), La Niña (Fig. 4b), and El Niño (Fig. 4c), with average silhouette widths of 0.29, 0.36, and 0.39, respectively. These values indicate that El Niño exhibits the best-defined clusters, with most points showing clear cohesion and separation, followed by La Niña with moderate clustering quality. In contrast, the neutral phase has the lowest silhouette width, reflecting significant overlap and less distinct cluster boundaries. While all phases have positive average silhouette widths, suggesting some degree of meaningful clustering, the relatively low values (all below 0.5) highlight challenges in achieving strong cluster separation, particularly for the neutral phase, which likely reflects greater variability in the data. This analysis underscores the varying complexity of precipitation or other climatic variables across different phases and suggests room for improvement in clustering optimization.

Figure 5 presents four maps showing the regionalization of Guatemala and surrounding areas based on different climatic phases: climatology (Fig. 5a), neutral (Fig. 5b), La Niña (Fig. 5c), and El Niño (Fig. 5d). The number of regions varies across phases, with eight regions for climatology, six for the neutral phase, and four for both El Niño and La Niña. This variation reflects the differing spatial complexities of precipitation or related variables, with the climatology showing the highest variability and El Niño and La Niña phases exhibiting more cohesive and predictable patterns. The neutral phase falls between these extremes, with moderate spatial variability requiring more clusters. These maps illustrate how climatic phases influence regional boundaries, emphasizing the importance of phase-specific regionalization to understand and manage climate impacts effectively.

3. Results

Precipitation was regionalized based on the analyzed phases, enabling the identification of distinct regions under specific conditions. Figure 5 illustrates the outcomes of this regionalization, detailing the composition of each region concerning the prevailing ENSO conditions and climatology. To explore these findings, the analysis will first evaluate the results within the context of the ENSO phases and climatology, supported by an ANOVA assessment. This will be followed by a detailed characterization of the identified regions and their unique features. Finally, the discussion will highlight the most significant insights into the regions' distinct climatic characteristics.

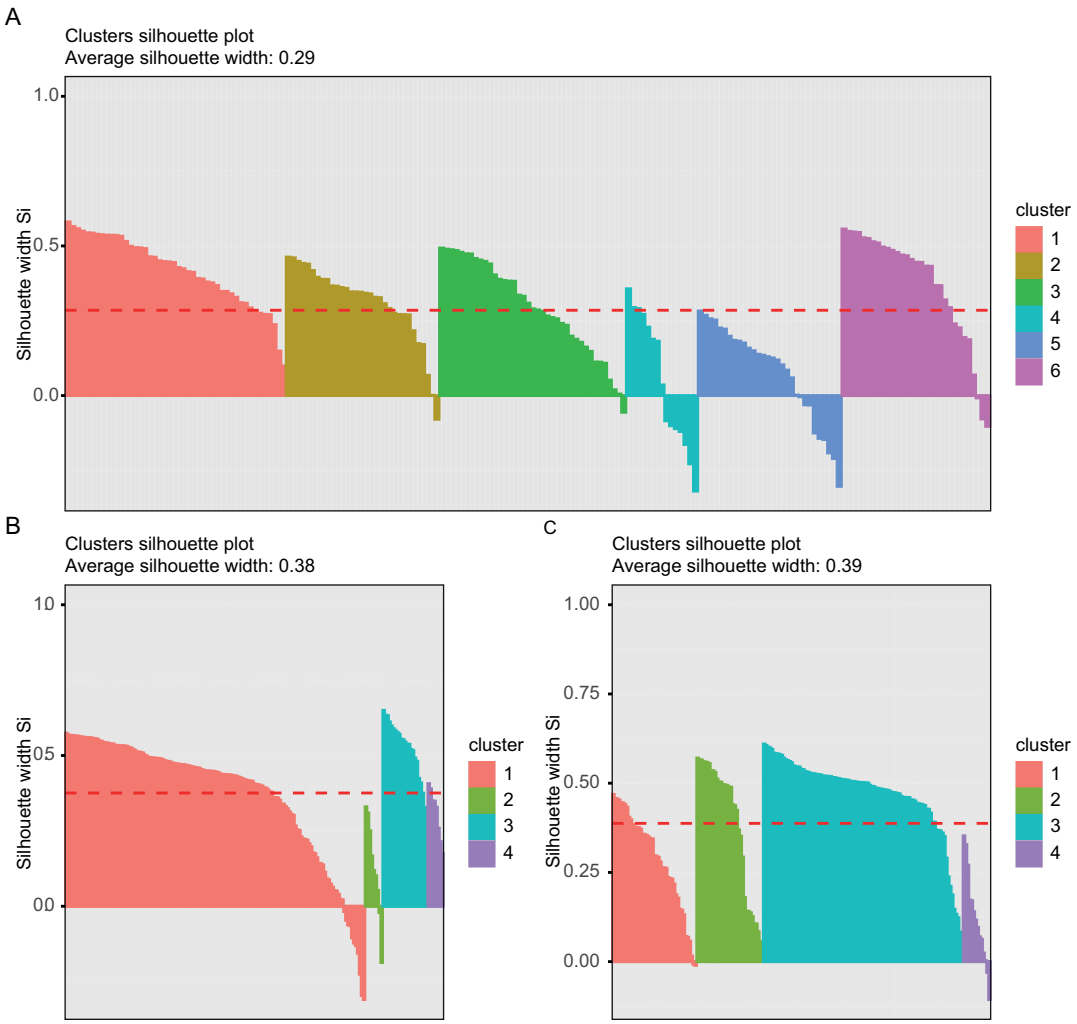

Fig. 4. (a) Mean Silhouette coefficient of the neutral phase; (b) mean Silhouette coefficient of the La Niña phase; (c) mean Silhouette coefficient of the El Niño phase.

3.1 Analysis of ENSO phases and climatology

Eight distinct regions regarding climatology were identified, representing the most detailed regionalization compared to other phases. This level of granularity reflects the inclusion of all available data across years, independent of ENSO conditions. The regions exhibit clear boundaries, with notable areas such as the Northern climatic region (Region 4), the Caribbean region (Region 3), and the Dry Corridor (Region 2). The central highlands and the Boca Costa region also appear as distinct regions (Regions 7 and 5, respectively). The diversity in these regions highlights Guatemala's complex climatic heterogeneity, and regions such as Region 6 (Northern Transversal Strip) and Region 1 (South Coast and eastern valleys) emerge as consistently distinct.

During the La Niña phase, four regions were identified, indicating a significant reduction in regional diversity. This simplification suggests more homogeneous climatic behavior under La Niña conditions. The areas closest to the Atlantic Ocean, such as Punta de Manabique and parts of the Northern Transversal Strip, maintain distinct characteristics. The Caribbean region (Region 3) and the southwestern mountains exhibit specific precipitation patterns, differing from the rest of the country. These changes highlight the dominant influence of La Niña, which appears to override finer climatic distinctions observed in other phases.

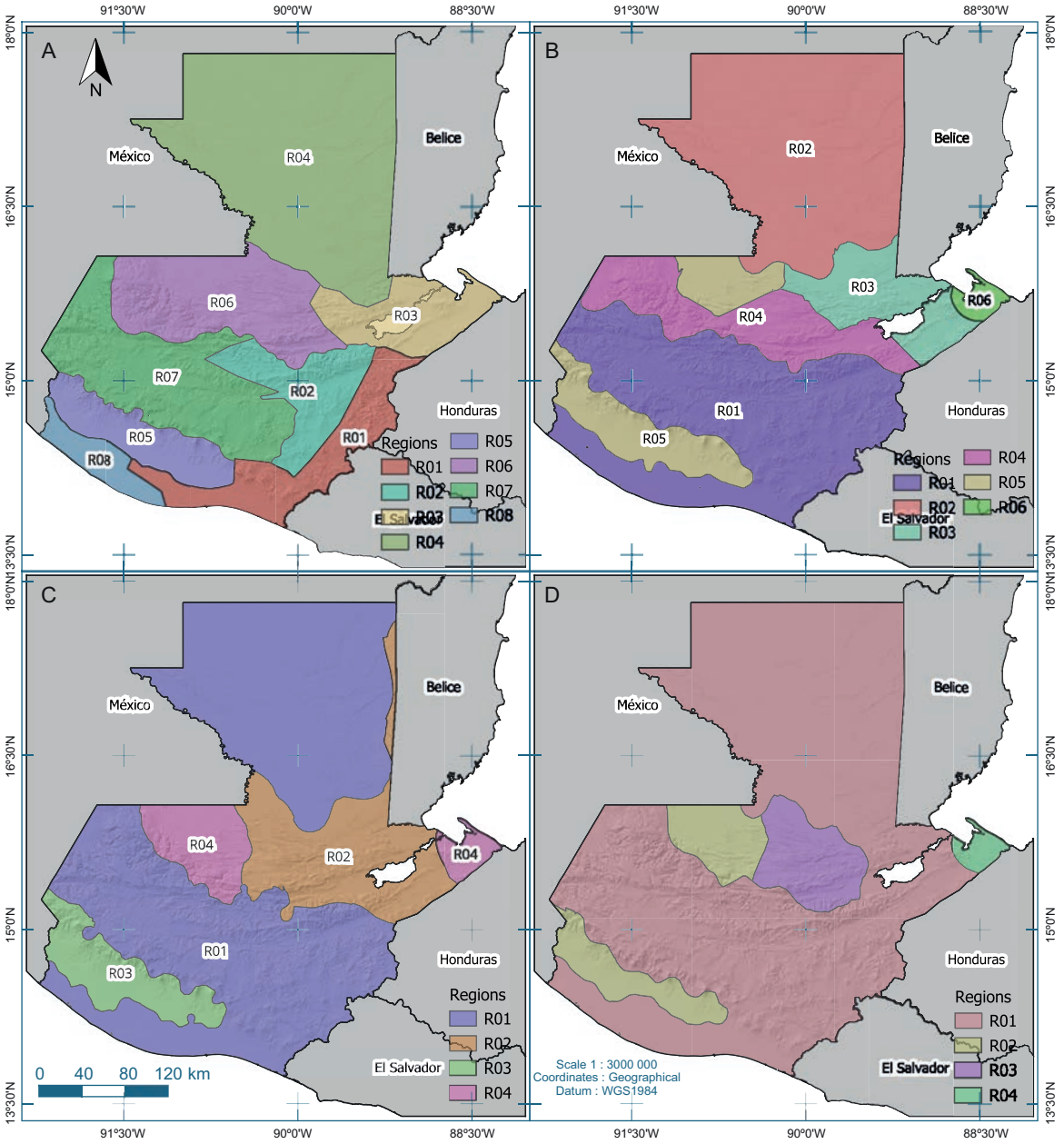

Fig. 5. Regionalization patterns: (a) climatology; (b) neutral ENSO phase; (c) La Niña ENSO phase; (d) El Niño ENSO phase. (Source: Mathematical Modelling and Research Unit, Faculty of Engineering, University of San Carlos de Guatemala.)

The El Niño phase also results in four distinct regions, like the La Niña phase, emphasizing generalized climatic behavior. However, the spatial distribution of regions differs slightly from La Niña, with more compact and clearly defined areas. Regions such as the Northern Transversal Strip and the South Coast exhibit generalized behavior, reflecting the overarching impact of El Niño conditions. Notably, the Dry Corridor (Region 2) appears to shrink, reflecting the influence of reduced precipitation typically associated with El Niño.

Across all phases, some regions, such as the Northern climatic region (Region 4) and the Caribbean region (Region 3), consistently appear, suggesting

they are robust climatic areas with distinct behaviors. These regions could be considered stable climatic zones, regardless of ENSO phase or climatology.

The climatology (Fig.5a) exhibits the most detailed regionalization, with eight regions, capturing the full variability of climatic conditions in Guatemala. In contrast, the ENSO phases (Fig. 5c, d) simplify the climatic landscape, reducing the regions to four, highlighting more generalized patterns. The neutral phase (Fig. 5b) sits between these extremes, with six regions, reflecting moderate climatic variability.

The observed changes in regional boundaries and the number of regions emphasize the influence of ENSO phases on Guatemala's precipitation patterns. While the climatology captures fine-scale variability, ENSO phases reveal how climatic conditions become more homogeneous under specific influences like El Niño and La Niña. These findings underscore the dynamic nature of Guatemala's climate and the need to consider phase-specific impacts for water resource management and agricultural planning.

When an ENSO phenomenon is observed, the regions are reduced, highlighting a different behavior. For example, in the case of La Niña, Figure 5c shows how certain areas with distinct behaviors persist. The area closest to the Atlantic Ocean, which includes Punta de Manabique and extends into the continental land of Guatemala, differs from the Northern Transversal Strip, the rest of the country, and the mountain range in the southwest. This results in four regions that exhibit similar behavior. A similar pattern occurs during the El Niño phase, as shown in Figure 5d, where four regions are identified, and the areas are reduced until a more generalized behavior emerges across different parts of the country. Additionally, the same four regions, which typically exhibit consistent behaviors across the different conditions analyzed (El Niño, La Niña, neutral, and climatology), are highlighted.

ENSO phases exert a profound influence on Guatemala's precipitation patterns, simplifying regional variability and altering boundaries. During La Niña, areas near the Atlantic Ocean, such as Punta de Manabique and the Northern Transversal Strip, experience distinct behavior due to increased rainfall. Conversely, El Niño reduces precipitation, leading to a contraction of regions like the Dry Corridor. These findings emphasize the critical role of ENSO in shaping climatic behavior, with significant implications for water management and disaster preparedness.

3.2 ANOVA analysis

The analysis examines annual rainfall variability across regions under different climatic phases (neutral, La Niña, and El Niño), as well as climatological conditions. Figure 6 illustrates the distribution of annual precipitation (mm) across eight regions (R01-R08), with significant differences identified by the ANOVA test ($p < 2.2e\text{-}16$). This figure highlights the variability in precipitation patterns across regions and climatic phases, emphasizing the distinct impacts of each phase on rainfall distribution.

While El Niño and La Niña phases share almost the same four regions, allowing for a general evaluation of precipitation variability between these opposite phases, their spatial extents are not entirely consistent. For instance, R4 remains on the Caribbean coast under both phases but expands to include an area bordering Chiapas, Mexico, during La Niña. Similarly, R3 differs between phases, with its boundaries under El Niño (turquoise) not aligning with those under La Niña (blue). These discrepancies introduce challenges in directly comparing rainfall variability between the two phases.

Climatology shows the highest variability in annual rainfall across regions, with eight distinct climatic zones. Region R06 consistently emerges as the wettest area, with median rainfall exceeding 4000 mm, reflecting its humid and stable precipitation patterns. On the other hand, regions R07 and R08 are the driest, with medians below 1500 mm, classifying them as semi-arid zones. This phase highlights the complex and heterogeneous nature of Guatemala's climate, capturing the full range of climatic diversity and providing a comprehensive baseline for understanding regional precipitation patterns.

In the neutral phase, the number of regions decreases slightly, and rainfall variability becomes less pronounced compared to the climatology. Region R06 remains the wettest, maintaining similar rainfall patterns as before, while other regions, such as R04 and R05, show slight reductions in precipitation. Regions R07 and R08 continue to exhibit the driest conditions. The neutral phase reflects an intermediate state where local climatic influences regain prominence, creating a balance between the detailed

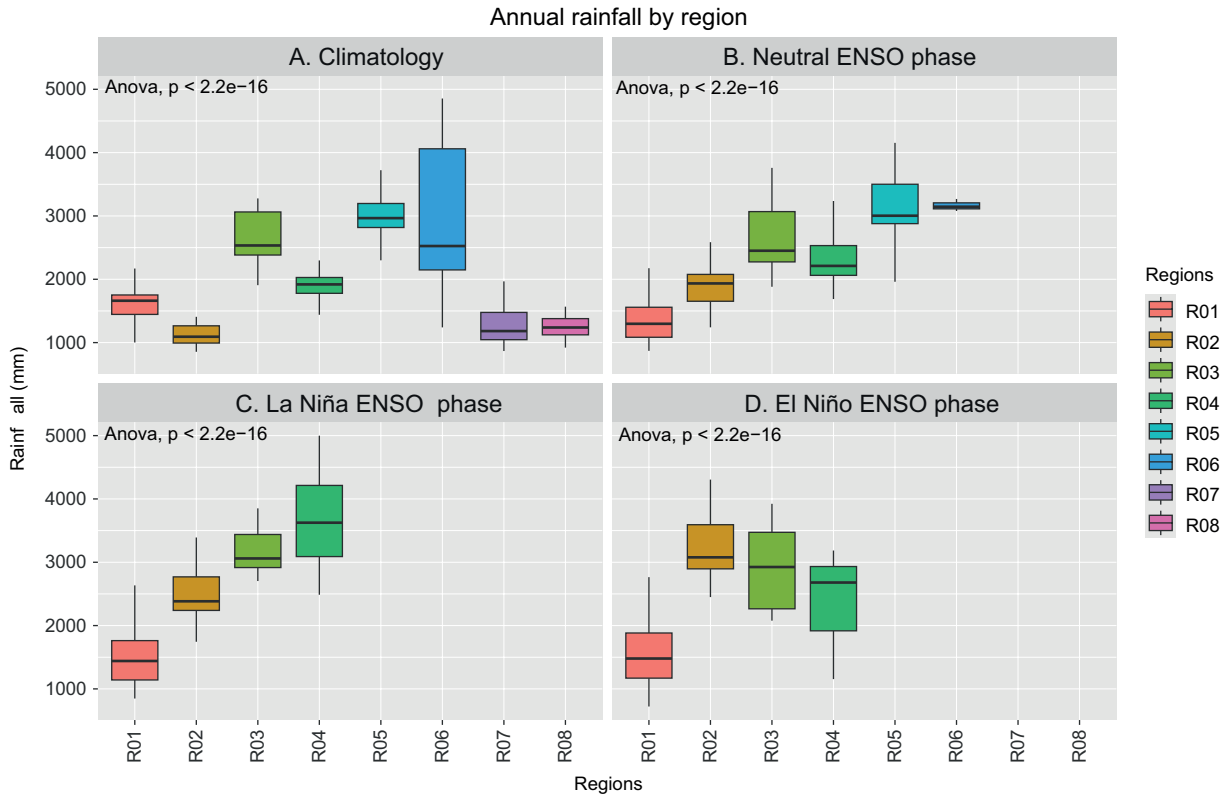

Fig. 6. Box plots of regionalization patterns: (a) climatology; (b) neutral ENSO phase; (c) La Niña ENSO phase; (d) El Niño ENSO phase.

variability of the climatology and the simplified patterns of ENSO phases.

The La Niña phase introduces significant shifts in rainfall patterns, with regions R03 and R04 receiving the highest rainfall, surpassing 4000 mm in median precipitation. This marks a redistribution of rainfall dominance from R06 to other regions influenced by La Niña's wetter conditions. Conversely, R01, R02, and R07 experience drier conditions, with R01 showing the lowest rainfall levels. La Niña's influence enhances rainfall in specific regions, leading to increased variability and potential flooding risks in areas such as R03 and R04.

El Niño phases result in a general suppression of rainfall across all regions, with reduced variability compared to other phases. Regions like R06 and R03 continue to receive relatively high rainfall, but to a lesser extent than in the climatology or neutral phases. Dry regions, such as R01, R02, and R07, experience even lower rainfall levels, emphasizing the drying effect of El Niño. This phase's homogenizing influence highlights its potential to exacerbate drought conditions, particularly in areas that already are arid or semi-arid.

A comparison of the phases highlights clear differences in rainfall levels and variability, as depicted by the box plots. Climatology captures the broadest variability, with well-defined wet (R06) and dry (R07, R08) regions. The neutral phase reduces this variability slightly, showing a more moderate rainfall distribution. In contrast, La Niña intensifies rainfall in specific regions, such as R03 and R04, leading to broader variability, while regions like R01 and R02 remain consistently dry. El Niño has the opposite effect, suppressing rainfall across most regions and narrowing variability, creating a more uniform and drier precipitation pattern.

The findings from the chart emphasize the dynamic influence of climatic phases on regional precipitation patterns in Guatemala. The climatology provides

the most comprehensive view of rainfall variability, while ENSO phases significantly alter these patterns. La Niña enhances precipitation and variability in wet regions, particularly R03 and R04, whereas El Niño suppresses rainfall and homogenizes variability across all regions. These results underscore the importance of tailoring water resource management strategies to specific phases, as the variability and distribution of rainfall differ markedly between phases, impacting both wet and dry regions.

3.3 Characterizations of the regions

Characterizing regions from a regionalization analysis is necessary because it provides a structured framework to understand spatial variability and climatic behavior across a given area. By defining distinct regions based on shared characteristics, regionalization allows researchers to identify patterns, trends, and anomalies that might otherwise be obscured in a broader analysis. The importance of this characterization lies in the careful selection and analysis of the variables that define these regions, as they capture key environmental, geographic or climatic factors influencing the area. Furthermore, it supports the interpretation of the regionalization process itself by validating the grouping of areas with similar conditions and highlighting transitions or boundaries that may warrant further investigation. This ensures that the results of regionalization are not only descriptive but also provide valuable insights into the underlying dynamics of the studied system.

Table III provides a detailed characterization of regions identified through regionalization analysis under different phases, such as El Niño. Each region

Table III. Regional characterization under El Niño, La Niña, neutral, and climatology conditions.

Phases analyzed	Region	Longitude geometric center (°W)	Latitude (°N)	Altitude (masl)	Area (km^2)	Precipitation minimum (mm $year^{-1}$)	Precipitation Maximum (mm $year^{-1}$)	Mean Precipitation (mm $year^{-1}$)	Standard Deviation (mm $year^{-1}$)	Longitude Minimum and maximum (°W)		Latitude (°N)		Distance to Pacific Ocean (km)	Distance to Atlantic Ocean (km)	Coefficient of variation
Niño	1	–90.506	15.225	887.80	89939.00	722.10	3992.40	1577.80	530.50	–88.2	–92.3	13.8	18.3	149.93	224.73	3.0
	2	–91.313	14.794	454.90	10355.50	2450.00	4981.20	3323.60	600.20	–90.6	–92.5	14.2	16.2	81.28	298.36	5.5
	3	–89.969	15.521	637.70	7262.40	2077.60	3923.00	2914.40	752.80	–89.7	–90.4	15.3	15.9	194.49	146.59	3.9
	4	–88.188	15.655	14.30	1368.40	1154.80	3185.40	2340.00	1057.10	–87.9	–88.6	15.5	15.8	289.51	3.50	2.2
Neutral	1	–90.726	14.69	1098.20	37422.90	869.60	2305.20	1342.40	321.50	–88.2	–92.1	13.8	16.3	92.30	231.95	4.2
	2	–89.696	17.103	139.20	35164.10	1241.30	2790.30	1915.90	385.20	–88.3	–91.5	16	18.3	363.90	148.56	5.0
	3	–89.310	15.696	212.60	10032.70	1881.60	3759.40	2651.10	610.40	–88.9	–89.8	15.4	16.1	232.15	53.75	4.3
	4	–90.644	15.522	1100.50	13059.50	1687.80	4562.10	2503.70	815.40	–89.2	–92.3	15.1	16.3	184.79	193.04	3.1
	5	–91.263	14.704	488.20	11914.70	1960.80	4923.60	3190.20	670.40	–90.3	–92.5	14.2	16.2	81.98	287.53	4.8
	6	–88.188	15.655	14.30	1331.40	3078.70	3268.30	3164.30	96.10	–87.9	–88.6	15.5	15.8	263.75	4.46	32.9
Niña	1	–90.688	15.096	956.20	81575.60	848.00	2871.90	1511.10	448.80	–88.2	–92.3	13.8	18.3	140.73	207.61	3.4
	2	–89.352	15.976	345.70	17963.50	1744.60	4253.80	2609.10	684.60	–88.3	–90.4	15.1	17.5	256.47	44.33	3.8
	3	–91.475	14.566	478.70	8037.80	2703.50	4776.40	3221.50	464.80	–90.8	–92.5	14.3	15.1	56.04	312.87	6.9
	4	–89.987	15.684	567.80	1345.70	1174.60	4999.10	3531.00	1133.00	–87.9	–91	15.4	16.2	236.05	114.36	3.1
Climatology	1	–90.410	14.231	390.40	10156.00	1002.00	2847.20	1652.30	361.50	–89.2	–91.4	13.8	15.2	39.59	273.41	4.6
	2	–90.083	14.976	1029.90	8036.60	855.00	2361.30	1227.60	408.70	–89.6	–90.7	14.3	15.3	127.94	191.09	3.0
	3	–89.285	15.560	126.80	8182.60	1906.90	3277.00	2635.70	472.10	–88.6	–89.8	15.4	15.8	221.89	75.34	5.6
	4	–90.018	16.653	199.70	37486.60	1326.90	2297.70	1870.40	264.20	–89.3	–90.9	15.7	17.6	307.98	169.81	7.1
	5	–91.300	14.481	499.60	7111.60	1524.90	4888.70	2988.50	637.10	–90.6	–92.1	14.1	14.9	51.45	305.86	4.7
	6	–90.625	15.587	1100.30	15520.20	1240.40	4854.80	3048.10	1123.30	–89.8	–91.4	15.3	16.1	190.84	189.74	2.7
	7	–91.112	15.000	1779.00	18976.00	867.00	3195.80	1339.40	461.30	–90.4	–92	14.4	15.9	115.53	253.65	2.9
	8	–91.766	14.370	31.70	3513.70	921.00	1991.10	1301.50	300.70	–91.2	–92.1	14	14.7	17.96	350.63	4.3

is described using variables that capture its spatial, physical, and climatic attributes. Geographical coordinates include the longitude and latitude of the geometric center as well as its minimum and maximum extents. Physical characteristics such as altitude (masl) and area (km²) provide insights into the region's topography. Precipitation metrics, including minimum, maximum, and mean annual precipitation (mm year^{-1}), standard deviation, and the coefficient of variation, highlight the variability and distribution of rainfall within each region. Additionally, distance metrics, such as proximity to the Pacific and Atlantic oceans (km), help contextualize the regions' climatic behavior. These variables collectively offer a comprehensive framework for analyzing regional differences and understanding the spatial and climatic dynamics across various phases.

Climatology captures a broad range of climatic data, providing a comprehensive baseline for analyzing rainfall variability. This phase has the highest mean precipitation (1,652.3 mm year^{-1}) and moderate standard deviation (361.5 mm year^{-1}), reflecting a balanced yet diverse rainfall distribution. The precipitation maximum is moderate compared to other phases (2847.2 mm year^{-1}), while the minimum precipitation is higher than in ENSO phases (1002 mm year^{-1}). The altitude in this phase averages 390.4 masl, with smaller regions averaging 10 156 km².

In the neutral phase, mean precipitation decreases (1342.4 mm year^{-1}) compared to climatology, with a slightly narrower standard deviation (321.5 mm year^{-1}), indicating less variability. The maximum (2305.2 mm year^{-1}) and minimum (869.6 mm year^{-1}) precipitation are also reduced, reflecting more stable yet subdued rainfall patterns. This phase is notable for having higher average altitudes (1098.2 masl) and larger regions (37 422.9 km² on average), suggesting a shift in regional dynamics where elevation and larger areas play a stronger role in modulating precipitation.

The La Niña phase highlights increased precipitation variability with a higher standard deviation (448.8 mm year^{-1}) and mean precipitation of 1511.1 mm year^{-1}. The maximum precipitation (2871.9 mm year^{-1}) is similar to the climatology, but the minimum precipitation (848 mm year^{-1}) is slightly lower. This phase emphasizes the wettest conditions in regions affected by La Niña, consistent with the phase's characteristic of enhancing rainfall. Regions in this phase are slightly smaller than in the neutral phase, with an average area of 81 575.6 km² and an average altitude of 956.2 masl, showing that mid-altitude regions experience intensified precipitation.

During the El Niño phase, suppressed rainfall is observed, with the lowest mean precipitation (1577.8 mm year^{-1}) and minimum precipitation (722.1 mm year^{-1}). Despite this, it shows the highest variability, with a standard deviation of 530.5 mm year^{-1} and maximum precipitation reaching 3992.4 mm year^{-1}, suggesting isolated regions receiving intense rainfall. This phase represents the driest conditions overall, highlighting the significant drying effects of El Niño. Regions under El Niño are the largest (89 939 km² on average) and are located at mid-altitudes (887.8 masl), emphasizing how regional size and elevation influence precipitation under this phase.

The analysis of these phases reveals significant insights into how regional climate is influenced by ENSO and other neutral conditions. Climatology provides a baseline for understanding Guatemala's diverse precipitation patterns, while the ENSO phases demonstrate the stark effects of global climatic phenomena. La Niña enhances rainfall variability, particularly in mid-altitude regions, whereas El Niño suppresses precipitation, creating drier conditions with occasional intense rainfall events. These findings highlight the importance of relating this information to regional characteristics, as it enables a deeper understanding of climatic dynamics and supports more targeted planning for water resources and disaster management in each phase.

Climatological analysis reveals variation in average monthly precipitation across the eight regions, highlighting a clear seasonality in rainfall distribution. Most regions exhibit a pronounced peak during the wettest months, typically between May and September, corresponding to the rainy season in Central America. However, there are notable differences in precipitation magnitudes between regions. For instance, Region 6 consistently receives higher rainfall across all months, particularly during the rainy season's peak, emphasizing its humid characteristics. In contrast, regions like 7 and 8 show lower monthly averages throughout the year, reflecting their semi-arid nature. This variability underscores the importance of understanding temporal rainfall patterns

to characterize the distinct climatic behavior of each region and its potential impacts on agriculture, water resources, and disaster preparedness.

Temporal analysis of climatological conditions provides spatial insights into annual precipitation patterns and regionalization of precipitation across the eight regions. In contrast, an overlay of interpolated annual rainfall data (Fig. S1 in the supplementary material) reveals finer details about the distribution and intensity of precipitation within and between regions. This integration is essential for explaining regional characteristics, since it combines spatial variability with temporal dynamics. For example, the interpolation highlights areas within Region 6 that receive extreme rainfall (above 4000 mm annually) and contrasts them with drier regions like 7 and 8, where annual totals are below 1500 mm. By incorporating temporal variation alongside spatial insights, the analysis offers a comprehensive understanding of regional precipitation dynamics, which is crucial for explaining the analysis phases and their implications for local climate management and planning.

Monthly average precipitation across six regions during the neutral phase showcases a distinct rainy season from May to October. Regions like 3 experience the highest precipitation, peaking above 600 mm during the wettest months, while Region 1 consistently receives the least rainfall, especially during the dry season from January to April. This temporal variability underscores the uneven distribution of rainfall across regions, emphasizing how localized climatic factors influence the intensity and duration of precipitation throughout the year. The differences between regions demonstrate the importance of understanding these temporal trends to address water availability and agricultural needs.

Spatial perspective on annual rainfall during the neutral phase complements this analysis, with additional details provided in associated maps and data (Fig. S2). One component defines the six regional boundaries based on shared climatic characteristics, while another overlay interpolated precipitation data, revealing internal variability within each region. For instance, Region 3 corresponds to areas receiving over 4000 mm annually, aligning with its high monthly rainfall patterns detailed in related datasets. In contrast, Region 1 falls within the driest zones, with annual precipitation below 1500 mm. By integrating temporal and spatial analyses, this approach captures both the seasonality and localized differences in rainfall, offering a comprehensive understanding of regional climatic behaviors during the neutral phase. This integration is essential for interpreting how these regions respond to specific climatic conditions.

Monthly average precipitation during the La Niña phase shows pronounced seasonality, with the highest rainfall between May and October, typical of the rainy season. Notably, Region 3 exhibits the highest monthly rainfall peaks, exceeding 500 mm in certain months, indicating its susceptibility to enhanced precipitation under La Niña conditions. Conversely, Region 1 consistently receives lower precipitation throughout the year, reflecting its drier characteristics. This variation highlights the differential impact of La Niña on rainfall distribution across regions, driven by localized factors such as topography and proximity to moisture sources. The monthly patterns emphasize the importance of analyzing temporal variability to understand the distinct responses of regions to La Niña's wetter conditions.

Spatial insights complement the temporal data, offering a clearer perspective on precipitation patterns (Fig. S3). One component illustrates the regionalization of the study area into four distinct regions based on shared climatic characteristics during the La Niña phase. When overlaid with interpolated annual rainfall data, the variation in precipitation intensity within each region becomes evident. For example, Region 3, identified as the wettest, corresponds to areas receiving over 4000 mm annually (highlighted in deep blue), while Region 1 aligns with drier zones receiving less than 1500 mm. This spatial overlay is crucial as it integrates temporal patterns with localized annual rainfall intensity, providing a more comprehensive understanding of each region's behavior under La Niña. This combined analysis enables targeted interventions and improved planning for water resource management and disaster preparedness in response to La Niña's climatic influence.

Monthly average precipitation during the El Niño phase highlights a distinct seasonal variation, with rainfall concentrated between May and October, the typical rainy season in Central America. Notably, Region 3 experienced the highest monthly rainfall, peaking at over 500 mm in September, while Region 1 remains the driest, with consistently lower precipitation throughout the year. The reduced intensity of

rainfall during the El Niño phase compared to the La Niña phase reflects the characteristic drying effect of El Niño, which tends to suppress precipitation across affected regions. This temporal variability underscores the importance of understanding how El Niño influences the distribution and intensity of rainfall throughout the year, shaping water availability and ecosystem dynamics.

Spatial context complements this temporal analysis by illustrating rainfall distribution during the El Niño phase. One component divides the study area into four regions based on shared climatic characteristics, while another overlays interpolated annual precipitation data to reveal localized variations within each region. For instance, Region 3, which exhibits the highest rainfall (Fig. S4), corresponds to areas receiving over 2500 mm annually (highlighted in blue), whereas Region 1, the driest region, aligns with areas receiving less than 1000 mm. This spatial overlay is crucial for understanding the regional impact of El Niño, as it integrates monthly variability with annual rainfall intensity. By combining temporal and spatial analyses, this approach provides a detailed picture of how El Niño influences regional precipitation patterns, enabling more effective planning for water resource management and disaster risk mitigation.

The analysis of the four sets of figures demonstrates the profound influence of climatology and ENSO phases (neutral, La Niña, and El Niño) on precipitation variability across regions. Each phase reveals distinct temporal and spatial patterns in rainfall, highlighting the dynamic nature of Guatemala's climate. Climatology captures the most comprehensive variability, serving as a baseline, while the neutral phase represents a moderate state with balanced rainfall distribution. In contrast, La Niña intensifies precipitation in specific regions, such as Region 3, leading to increased rainfall variability, while El Niño suppresses overall rainfall, creating drier conditions with localized extremes. Combining monthly temporal patterns with spatial interpolations of annual precipitation underscores the importance of integrating both perspectives to fully understand regional responses to different climatic conditions.

3.4. Essential variables for regional description

Considering variables like annual precipitation and distance to the Pacific Ocean is essential for the regional description because these factors directly influence the spatial and climatic behavior of regions. Precipitation is a critical variable for understanding water availability, agricultural potential, and ecosystem dynamics, while the distance to the Pacific Ocean helps to explain how proximity to moisture sources impacts rainfall patterns. These variables capture spatial variability and the interactions between geographic features and climatic processes, offering a nuanced understanding of regional behavior.

In Figure 7a, the relationship between annual precipitation and the distance to the Pacific Ocean during the El Niño phase reveals a strong negative correlation (R^2 = 0.9785), indicating that regions closer to the Pacific Ocean receive significantly more rainfall. For example, Region 2 in the El Niño phase, located approximately 50 km from the ocean, records the highest annual precipitation of around 3750 mm. In contrast, Region 4 in the El Niño phase, located over 300 km from the coast, receives significantly less rainfall, at approximately 2250 mm. The regression equation ($y = 4.6886x + 3742.8$) highlights this decreasing trend, where precipitation diminishes by approximately 4.7 mm for every kilometer of increased distance from the Pacific. This strong correlation underscores the pronounced impact of proximity to the Pacific Ocean on precipitation distribution during El Niño, likely influenced by reduced moisture availability as distance increases.

In Figure 7b, the relationship between annual precipitation and distance to the Pacific Ocean during the La Niña phase shows a weaker positive correlation (R^2 = 0.644), reflecting a different dynamic than El Niño. Here, Region 1 in the La Niña phase, located closest to the ocean, has the lowest precipitation (around 2000 mm), while Region 4 in the La Niña phase, located about 250 km away, receives the highest precipitation (approximately 3500 mm). The regression equation ($\gamma = 13.136x - 222.37$) indicates an increase in precipitation of approximately 13.1 mm per kilometer of distance from the Pacific Ocean. This pattern suggests that during La Niña, inland regions benefit more from enhanced moisture transport, possibly due to intensified atmospheric dynamics and regional rainfall patterns. The contrasting tendencies between the two phases highlight how El Niño and La Niña influence rainfall differently, driven by changes in moisture transport mechanisms and the spatial dynamics of precipitation.

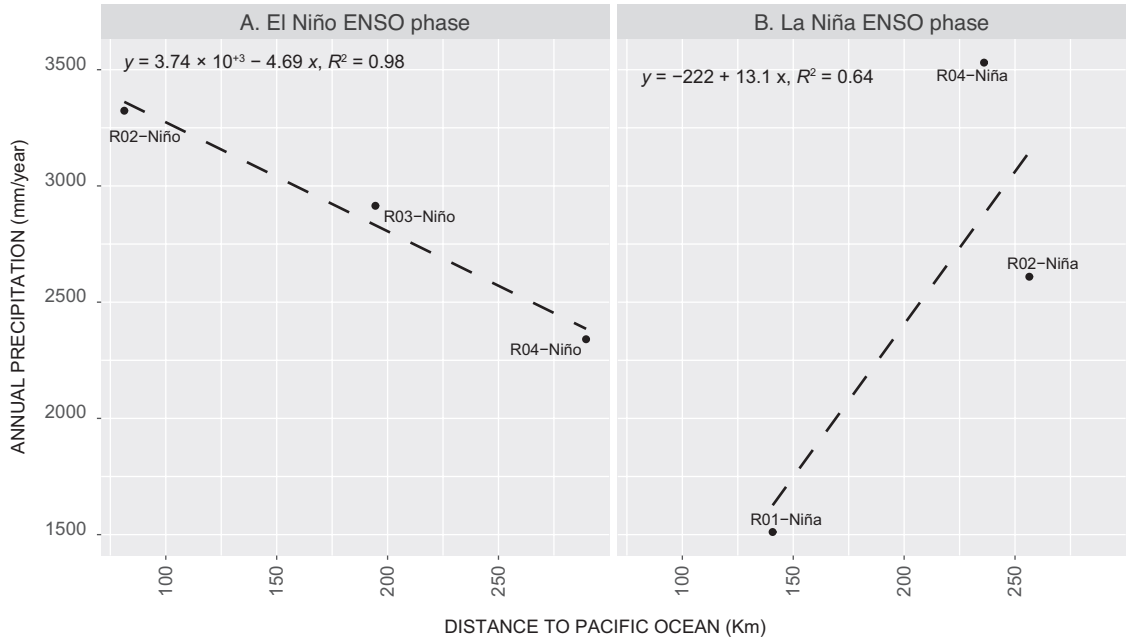

Fig. 7. (a) Annual precipitation and distance to the Pacific Ocean during El Niño phase; (b) annual precipitation and distance to the Pacific Ocean during La Niña phase. (Source: own elaboration.)

Moreover, the contrasting correlations observed during El Niño and La Niña phases highlight how these variables reflect phase-specific climatic responses. For instance, during El Niño, closer proximity to the Pacific Ocean corresponds to higher rainfall due to moisture concentration near the coast. In contrast, during La Niña, inland regions may receive more precipitation due to enhanced atmospheric moisture transport.

In Figure 8a, the correlation between annual precipitation and distance to the Atlantic Ocean during the neutral phase demonstrates a moderate negative relationship ($R^2 = 0.7197$). The regression equation ($y = 6.264x + 3107$) indicates that precipitation decreases by approximately 6.26 mm for every kilometer of increased distance from the Atlantic Ocean. Region 6 in the neutral phase, located closest to the Atlantic Ocean (around 50 km), experiences the highest annual precipitation, exceeding 3000 mm. Conversely, Region 1 in the neutral phase, the farthest from the Atlantic Ocean (around 200 km), receives the least precipitation, around 1200 mm. This pattern highlights the critical role of the Atlantic Ocean as a moisture source during the neutral phase, where proximity to the ocean significantly impacts precipitation distribution.

In Figure 8b, the relationship between annual precipitation and distance to the Pacific Ocean during the neutral phase reveals a strong positive correlation ($R^2 = 0.9451$), with precipitation increasing as regions move farther from the Pacific Ocean. The regression equation ($y = 9.976x + 502.62$) suggests an increase of nearly 10 mm in annual precipitation for every kilometer of increased distance from the Pacific. Region 1 in the neutral phase, closest to the Pacific, records the lowest precipitation (approximately 1200 mm), while Region 4 in the neutral phase, located over 200 km from the Pacific, receives the highest precipitation (around 2500 mm). This opposite trend compared to the Atlantic Ocean reflects the differential influence of oceanic moisture sources on precipitation under neutral conditions.

These variables are essential for regional description because they illustrate how geographic proximity to major moisture sources influences precipitation patterns, especially under neutral phase conditions. The contrasting correlations with the Atlantic and Pacific oceans highlight the complexity of

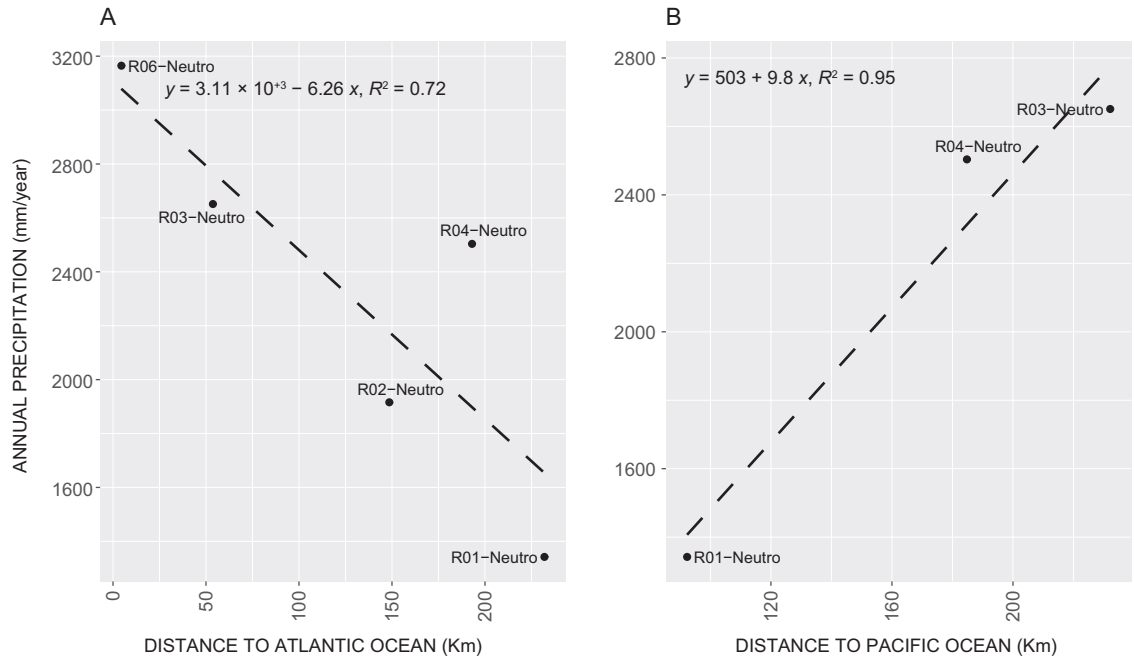

Fig. 8. (a) Annual precipitation and distance to Atlantic Ocean during neutral conditions; (b) annual precipitation and distance to Pacific Ocean during neutral conditions.

Guatemala's climate dynamics, where precipitation is not uniformly distributed but shaped by the interactions of topography and oceanic influences.

In Figure 9a, the relationship between annual precipitation and distance to the Atlantic Ocean under climatology shows a moderate negative correlation ($R^2 = 0.5603$). The regression equation ($y = 5.425x + 2809$) indicates that precipitation decreases by approximately 5.43 mm for every kilometer of increased distance from the Atlantic Ocean. Region 3 in climatology conditions, located closest to the Atlantic Ocean at approximately 50 km, receives the highest precipitation, around 2800 mm annually. In contrast, Region 1 in climatology, the farthest from the Atlantic at nearly 250 km, receives the lowest annual precipitation, approximately 1500 mm. This trend emphasizes the influence of proximity to the Atlantic Ocean as a primary moisture source, with precipitation decreasing as distance increases.

In Figure 9b, the relationship between annual precipitation and distance to the Pacific Ocean demonstrates a stronger positive correlation ($R^2 = 0.7767$) under climatology. The regression equation ($y = 46.201x + 302.12$) indicates that precipitation increases by approximately 46.2 mm for every kilometer farther from the Pacific Ocean. Region 5 in climatology conditions, located about 50 km from the Pacific, receives the highest precipitation, approximately 3000 mm annually. Conversely, Region 1 in climatology, the closest to the Pacific, records the lowest precipitation, around 1500 mm annually. This strong positive trend highlights the Pacific Ocean's more localized influence on precipitation, with regions farther away benefiting from greater rainfall accumulation likely due to topographical effects or broader atmospheric patterns that transport moisture inland.

When comparing the two relationships, the Atlantic Ocean's influence appears more widespread but less strongly correlated with precipitation trends, likely due to the moderating effects of distance and topographical variation. Conversely, the Pacific Ocean shows a stronger and more localized impact, emphasizing the importance of inland transport mechanisms and elevation in shaping rainfall. Together, these trends highlight the interplay of proximity to moisture sources, topographical barriers, and atmospheric dynamics in defining regional precipitation patterns under climatology.

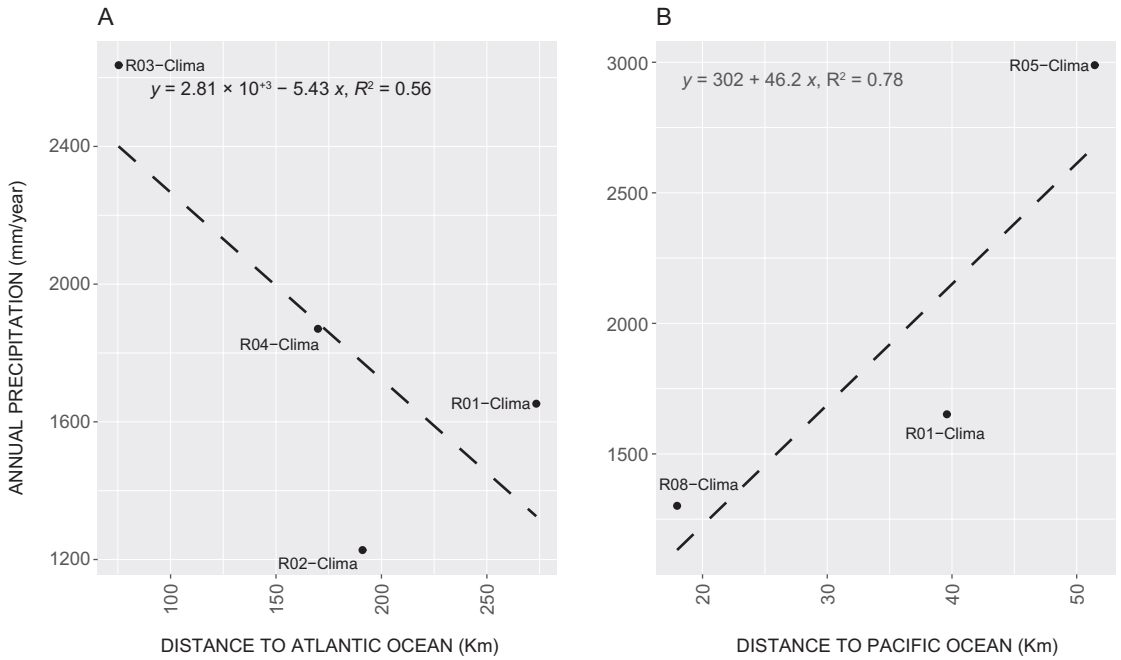

Fig. 9. (a) Annual precipitation and distance to Atlantic Ocean in climatology conditions; (b) annual precipitation and distance to Pacific Ocean in climatology conditions.

4. Discussion and conclusions

This study provides valuable insights into the regionalization of precipitation across climatology and ENSO phases (El Niño, La Niña, and neutral) in Guatemala. Climatology exhibited the highest regional and temporal variability, identifying eight distinct regions and serving as a comprehensive baseline for understanding the country's precipitation dynamics. ENSO phases significantly modified these patterns, with La Niña enhancing rainfall variability and increasing precipitation in regions such as the Northern Transversal Strip, while El Niño suppressed rainfall, creating drier conditions and localized extremes. Neutral phases displayed intermediate behavior, characterized by moderate variability and stable rainfall patterns.

The findings highlight the critical role of dynamic climatic boundaries in capturing the complexity of precipitation variability. Unlike traditional studies, such as those by Magaña et al. (2003) and Kolivras and Comrie (2007), which often treat climatic regions as static, this study demonstrates that regional boundaries in Guatemala shift depending on ENSO phases and local climatic factors. For instance, during La Niña, regions like the central Northern Transversal Strip expand due to increased precipitation, while during El Niño, these regions contract. This dynamic framework aligns with recent perspectives, such as those by Hidalgo et al. (2013), emphasizing the importance of phase-dependent regional shifts in understanding climatic systems.

The interplay between topography and proximity to moisture sources emerged as a key driver of precipitation distribution. The southwestern volcanic highlands maintained stable precipitation patterns due to their altitude and consistent weather systems, rendering them less affected by ENSO. In contrast, regions near the Atlantic Ocean, such as Izabal, experienced enhanced precipitation during La Niña phases due to their proximity to moisture sources. Similarly, the Northern Transversal Strip demonstrated dual behavior: its northern portion remained relatively stable, while its central portion exhibited greater variability, expanding or contracting depending on climatic phases. These findings align with studies such as Rau et al. (2017) and Ilbay-Yupa et al. (2021), which similarly noted the influence of topography and moisture sources in

shaping precipitation patterns in other regions of Central and South America.

The practical implications of these findings are significant for agriculture, water resource management, and disaster preparedness. Identifying stable regions, such as the southwestern highlands, provides a foundation for long-term planning, while understanding the variability of regions like the Northern Transversal Strip can guide adaptive strategies during extreme ENSO events. By offering a flexible and dynamic framework, this study moves beyond static models, addressing critical challenges in managing climatic variability and ensuring more accurate predictions for sustainable development.

Despite its contributions, the study acknowledges certain limitations. The analysis primarily focuses on precipitation as a single climatic variable, excluding temperature, anthropogenic factors such as land use, and soil moisture characteristics, which could offer a more comprehensive understanding of climatic impacts. Additionally, while the resolution of regional boundaries is robust, finer-scale topographical data and advanced modeling techniques could further improve the precision of the results. Incorporating these factors in future research would refine predictive models and strengthen the ability to adapt to evolving climatic conditions.

Future studies should explore the integration of additional climatic variables, such as temperature, soil moisture, and land use changes, to provide a more holistic understanding of Guatemala's climate dynamics. Advanced modeling techniques, such as combining k-means clustering with regional vector methods as proposed by Rau et al. (2017), could further enhance the accuracy of regional boundary definitions. Additionally, research could draw from Jupin et al. (2023), whose work on precipitation trends and variability in the Usumacinta River basin underscores the importance of homogenized datasets and cross-border climatic influences. Their approach highlights the critical role of Atlantic moisture sources, which could further contextualize precipitation patterns in Guatemala, particularly in transboundary regions like the Dry Corridor and Northern Transversal Strip. Investigating the long-term impacts of climate change on precipitation patterns and regional boundaries will also be crucial for informing sustainable resource management and climate adaptation strategies.

References

Al-Qadami A, Abdulla FA. 2019. Regionalization of precipitation in Jordan. In: Patterns and mechanisms of climate, paleoclimate and paleoenvironmental changes from low-latitude regions (Zhang Z, Khélifi N, Mezghani A, Heggy E, Eds.). CAJG 2018: Advances in Science, Technology & Innovation. Springer, Cham, 115-118. https://doi.org/10.1007/978-3-030-01599-2_27

Amador JA. 2008. The Intra-Americas Sea Low-Level Jet: Overview and future research. Annals of the New York Academy of Sciences 1146: 153-188. https://doi.org/10.1196/annals.1446.012

Bardales-Espinoza AW, Castañón C, Herrera-Herrera JL. 2019. Clima de Guatemala, tendencias observadas e índices de cambio climático. In: Primer reporte de evaluación del conocimiento sobre cambio climático en Guatemala (Castellanos EJ, Paiz-Estévez A, Escribá J, Rosales-Alconero M, Santizo A, Eds.). Editorial Universitaria UVG, Guatemala. Available at: https://sgccc.org.gt/wp-content/uploads/2019/07/1RepCCGuaCap2.pdf (accessed October 15, 2024).

Bell GD, Chelliah M. 2006. Leading tropical modes associated with interannual and multidecadal fluctuations in North Atlantic hurricane activity. Journal of Climate 19: 590-612. https://doi.org/10.1175/JCLI3659.1

Bhatia N, Sojan JM, Simonovic S, Srivastav R. 2020. Role of cluster validity indices in delineation of precipitation regions. Water 12: 1372. https://doi.org/10.3390/W12051372

Cane MA, Zebiak SE. 1985. A theory for El Niño and the Southern Oscillation. Science 228: 1085-1087. https://doi.org/10.1126/science.228.4703.1085

Chen AA, Taylor MA. 2002. Investigating the link between early season Caribbean rainfall and the El Niño+1 year. International Journal of Climatology 22: 87-106. https://doi.org/10.1002/joc.711

Darand M, Mansouri Daneshvar M. 2014. Regionalization of precipitation regimes in Iran using principal component analysis and hierarchical clustering analysis. Environmental Processes 1: 517-532. https://doi.org/10.1007/s40710-014-0039-1

De la Barreda B, Metcalfe SE, Boyd DS. 2020. Precipitation regionalization, anomalies and drought occurrence in the Yucatan Peninsula, Mexico. International Journal of Climatology 40: 4541-4555. https://doi.org/10.1002/joc.6474

Funk C, Peterson P, Landsfeld M, Pedreros D, Verdin J, Shukla S, Husak G, Rowland J, Harrison L, Hoell A,

Michaelsen J. 2015. The climate hazards infrared precipitation with stations – A new environmental record for monitoring extremes. Scientific Data 2: 150066. https://doi.org/10.1038/sdata.2015.66

Gomes EP, Blanco CJC, Pessoa FCL. 2018. Regionalization of precipitation with determination of homogeneous regions via fuzzy C-means. Revista Brasileira de Recursos Hídricos 23: e51. https://doi.org/10.1590/2318-0331.231820180079

Hidalgo HG, Amador JA, Alfaro EJ, Quesada B. 2013. Hydrological climate change projections for Central America. Journal of Hydrology 495: 94-112. https://doi.org/10.1016/j.jhydrol.2013.05.004

Hilario F, de Guzmán R, Ortega D, Hayman P, Alexander B. 2009. El Niño Southern Oscillation in the Philippines: Impacts, forecasts, and risk management. Philippine Journal of Development 36: 9-34.

Ilbay ML, Zubieta-Barragán R, Lavado-Casimiro W. 2019. Regionalization of precipitation, its aggressiveness and concentration in the Guayas River basin, Ecuador. La Granja: Revista de Ciencias de la Vida 30: 52-69. https://doi.org/10.17163/lgr.n30.2019.06

Ilbay-Yupa M, Lavado-Casimiro W, Rau P, Zubieta R, Castillón F. 2021. Updating regionalization of precipitation in Ecuador. Theoretical and Applied Climatology 143: 1513-1528. https://doi.org/10.1007/s00704-020-03476-x

Jupin JLJ, García-López AA, Briceño-Zuluaga FJ, Sifeddine A, Ruiz-Fernández AC, Sánchez-Cabeza, JA, Cardoso-Mohedano JG. 2023. Precipitation homogenization and trends in the Usumacinta River basin (Mexico-Guatemala) over the period 1959-2018. International Journal of Climatology 44:108-125. https://doi.org/10.1002/joc.8318

Kolivras KN, Comrie AC. 2007. Regionalization and variability of precipitation in Hawaii. Physical Geography 28: 76-96. https://doi.org/10.2747/0272-3646.28.1.76

Li-Juan C, De-Liang C, Hui-Jun W, Jing-Hui Y. 2009. Regionalization of precipitation regimes in China. Atmospheric and Oceanic Science Letters 2: 301-307. https://doi.org/10.1080/16742834.2009.11446818

Liu L, Xu ZX. 2016. Regionalization of precipitation and the spatiotemporal distribution of extreme precipitation in southwestern China. Natural Hazards 80: 1195-1211. https://doi.org/10.1007/s11069-015-2018-x

Magaña VO, Vázquez JL, Pérez JL, Pérez JB. (2003). Impact of El Niño on precipitation in Mexico. Geofísica Internacional 42: 313-330.

Maldonado T. 2016. Inter-annual variability of rainfall in Central America: Connection with global and regional climate modulators. Digital Comprehensive Summaries of Uppsala Dissertations from the Faculty of Science and Technology, Uppsala University, 67 pp.

Maldonado T, Rutgersson A, Alfaro E, Amador J, Claremar B. 2016. Interannual variability of the midsummer drought in Central America and the connection with sea surface temperatures. Advances in Geosciences 42: 35-50. https://doi.org/10.5194/adgeo-42-35-2016

Meddi M, Meddi H, Toumi S, Mehaiguen M. 2013. Regionalization of rainfall in north-western Algeria. Geographia Technica 17: 56-69.

Miller JA, Goodrich GB. 2007. Regionalization and trends in winter precipitation in the northwestern USA. Climate Research 33: 215-227. https://doi.org/10.3354/cr033215

Parrett C. 1998. Regionalization of precipitation characteristics in Montana using L-moments. Transportation Research Record: Journal of the Transportation Research Board 1647: 43-52. https://doi.org/10.3141/1647-06

Penalba OC, Rivera JA. 2016. Precipitation response to El Niño/La Niña events in southern South America – Emphasis in regional drought occurrences. Advances in Geosciences 42: 1-14. https://doi.org/10.5194/adgeo-42-1-2016

Poveda G, Mesa OJ. 2000. On the existence of Lloró (the rainiest locality on Earth): Enhanced Ocean-land-atmosphere interaction by a low-level jet. Geophysical Research Letters 27:1675-1678. https://doi.org/10.1029/1999GL006091

Raja NB, Aydin O. 2019. Regionalization of precipitation in Mauritius: A statistical approach. Meteorological Applications 26: 711-719. https://doi.org/10.1002/met.1798

Rau P, Bourrel L, Labat L, Melo P, Dewitte B, Frappart F, Lavado W, Felipe O. 2017. Regionalization of rainfall over the Peruvian Pacific slope and coast. International Journal of Climatology 37: 143-158. https://doi.org/10.1002/joc.4693

Raziei T. 2017. A precipitation regionalization and regime for Iran based on multivariate analysis. Theoretical and Applied Climatology 131: 1429-1448. https://doi.org/10.1007/s00704-017-2065-1

Rousseeuw PJ. 1987. Silhouettes: A graphical aid to the interpretation and validation of cluster analysis. Journal of Computational and Applied Mathematics 20: 53-65. https://doi.org/10.1016/0377-0427(87)90125-7

Santos EB, Lucio PS, Silva CMS. 2015. Precipitation regionalization of the Brazilian Amazon. Atmospheric Science Letters 16: 185-192. https://doi.org/10.1002/asl2.535

Satyanarayana P, Srinivas VV. 2011. Regionalization of precipitation in data sparse areas using large scale atmospheric variables – A fuzzy clustering approach. Journal of Hydrology 405: 462-473. https://doi.org/10.1016/j.jhydrol.2011.05.044

Shi P, Sun S, Wang M, Li N, Wang J, Jin Y, Gu X, Yin W. 2014. Climate change regionalization in China (1961-2010). Science China Earth Sciences 57: 2676-2689. https://doi.org/10.1007/s11430-014-4889-1

Srinivas VV. 2013. Regionalization of precipitation in India – A review. Journal of the Indian Institute of Science 93:153-162.

Wang C. 2007. Variability of the Caribbean Low-Level Jet and its relations to climate. Climate Dynamics 29: 411-422. https://doi.org/10.1007/s00382-007-0243-z

Zhang Y, Moges S, Block P. 2016. Optimal cluster analysis for objective regionalization of seasonal precipitation in regions of high spatial-temporal variability: Application to western Ethiopia. Journal of Climate 29: 3697-3717. https://doi.org/10.1175/JCLI-D-15-0582.1

SUPPLEMENTARY MATERIAL

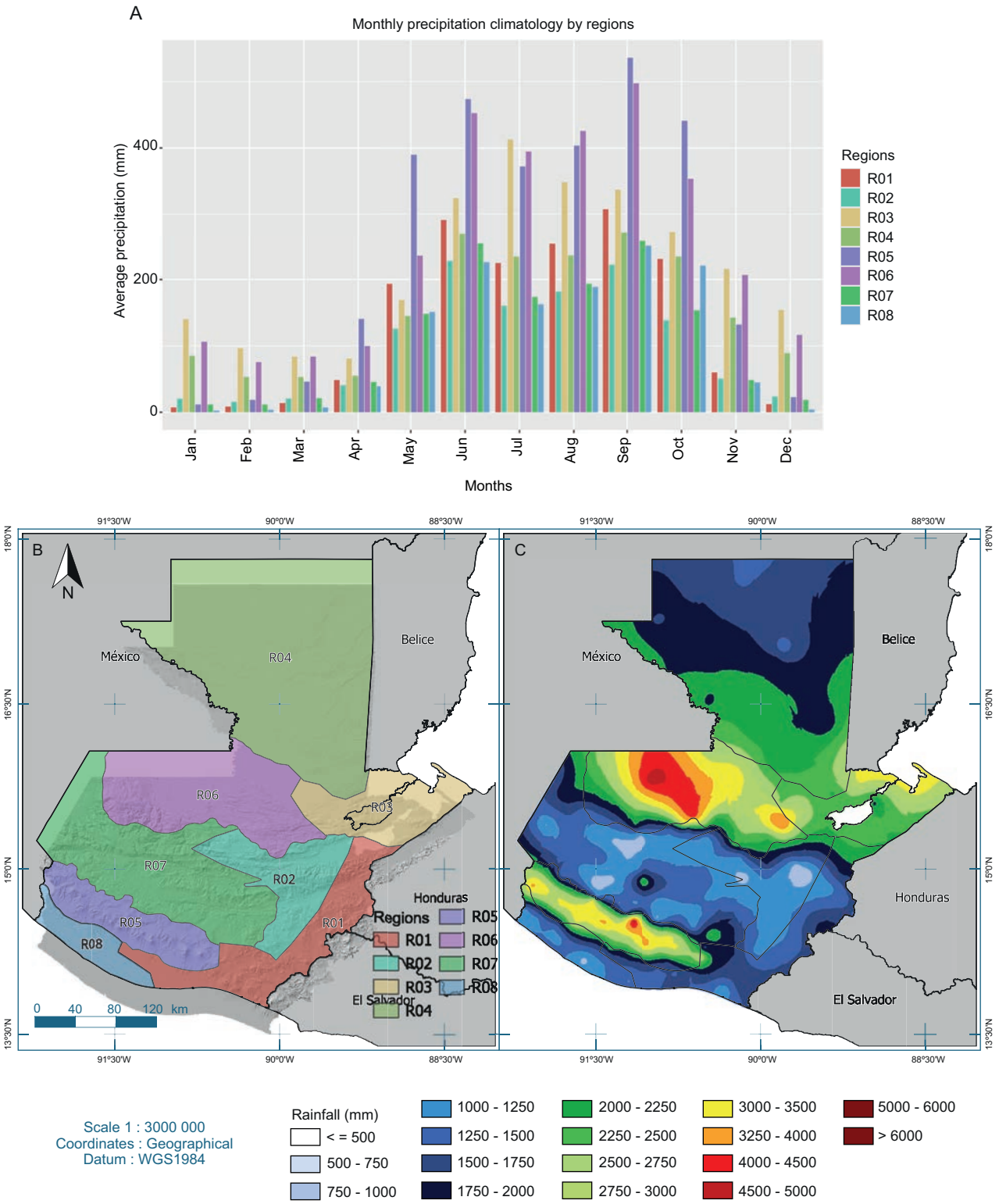

Fig. S1. (a) Climatology regions and average monthly precipitation; (b) climatology regions and their boundaries; (c) average annual precipitation of the climatology approach and regions boundaries. (Source: Mathematical Modelling and Research Unit, Faculty of Engineering, University of San Carlos de Guatemala.)

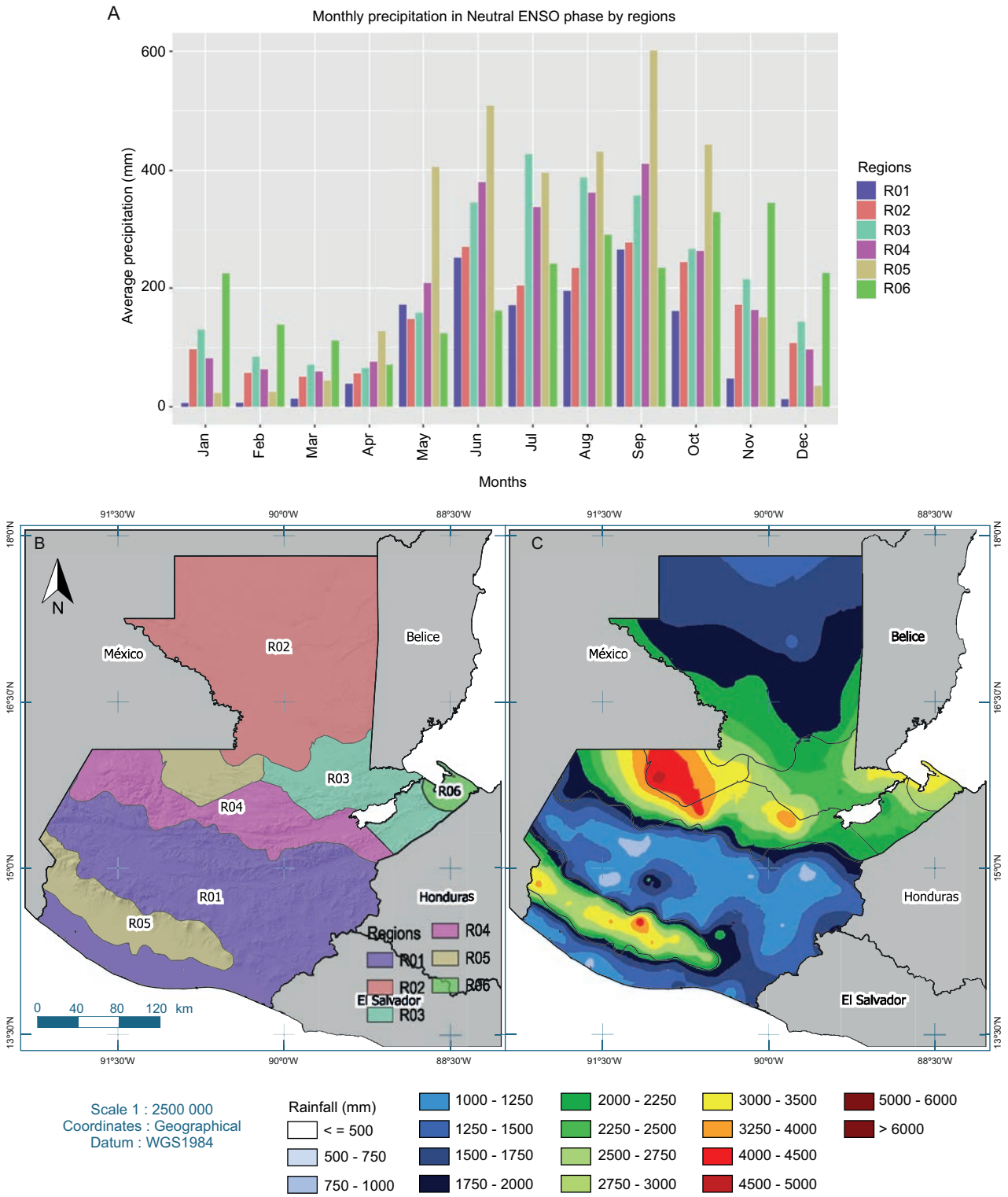

Fig. S2. (a) Regions and average monthly precipitation under neutral conditions; (b) neutral conditions climate regions and its boundaries; (c) average annual precipitation under neutral conditions and regions boundaries. (Source: Mathematical Modelling and Research Unit, Faculty of Engineering, University of San Carlos de Guatemala.)

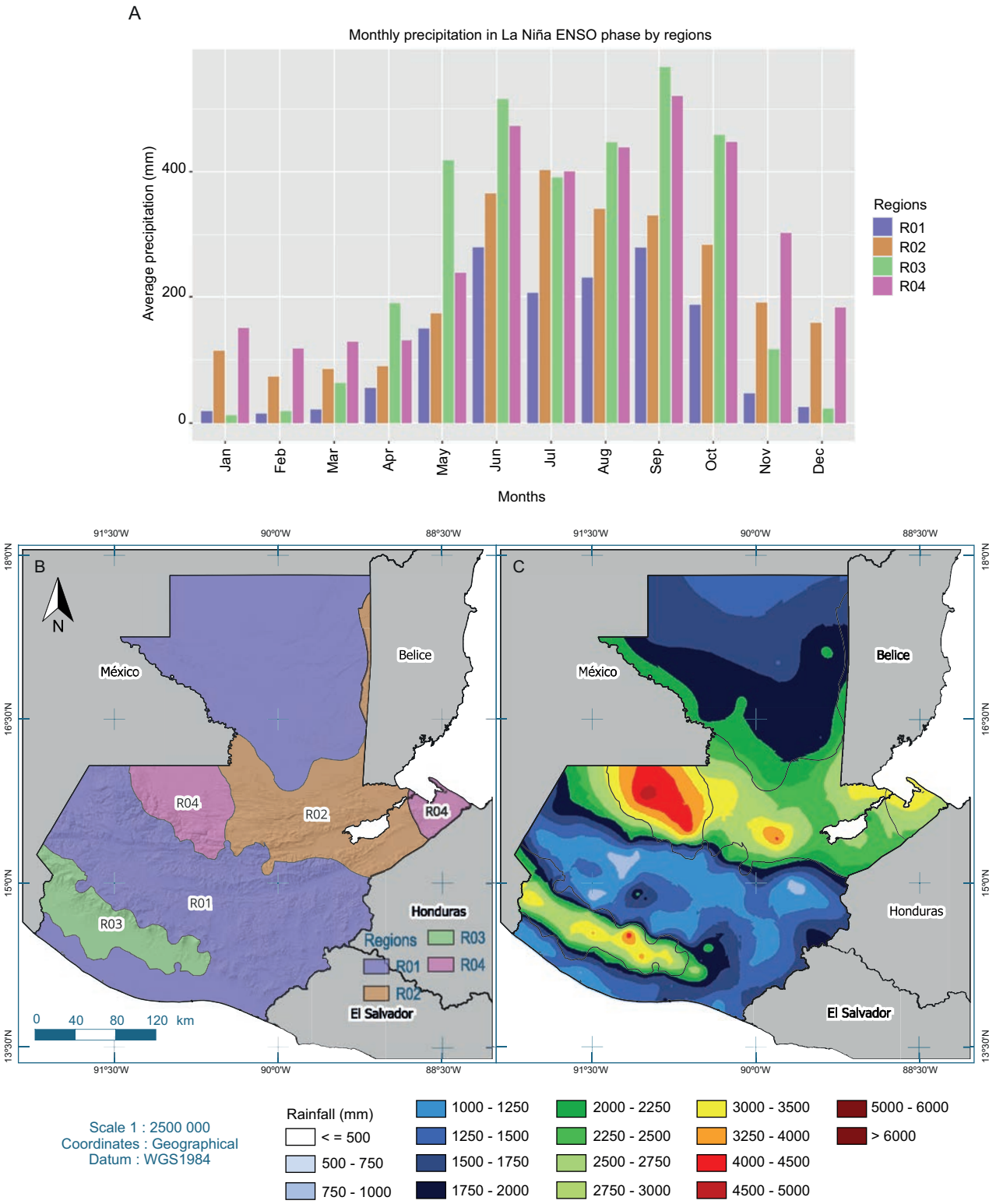

Fig. S3. (a) Regions and average monthly precipitation under La Niña conditions; (b) climate regions and their boundaries under La Niña conditions; (c) average annual precipitation under La Niña conditions and regions' boundaries. (Source: Mathematical Modelling and Research Unit, Faculty of Engineering, University of San Carlos de Guatemala.)

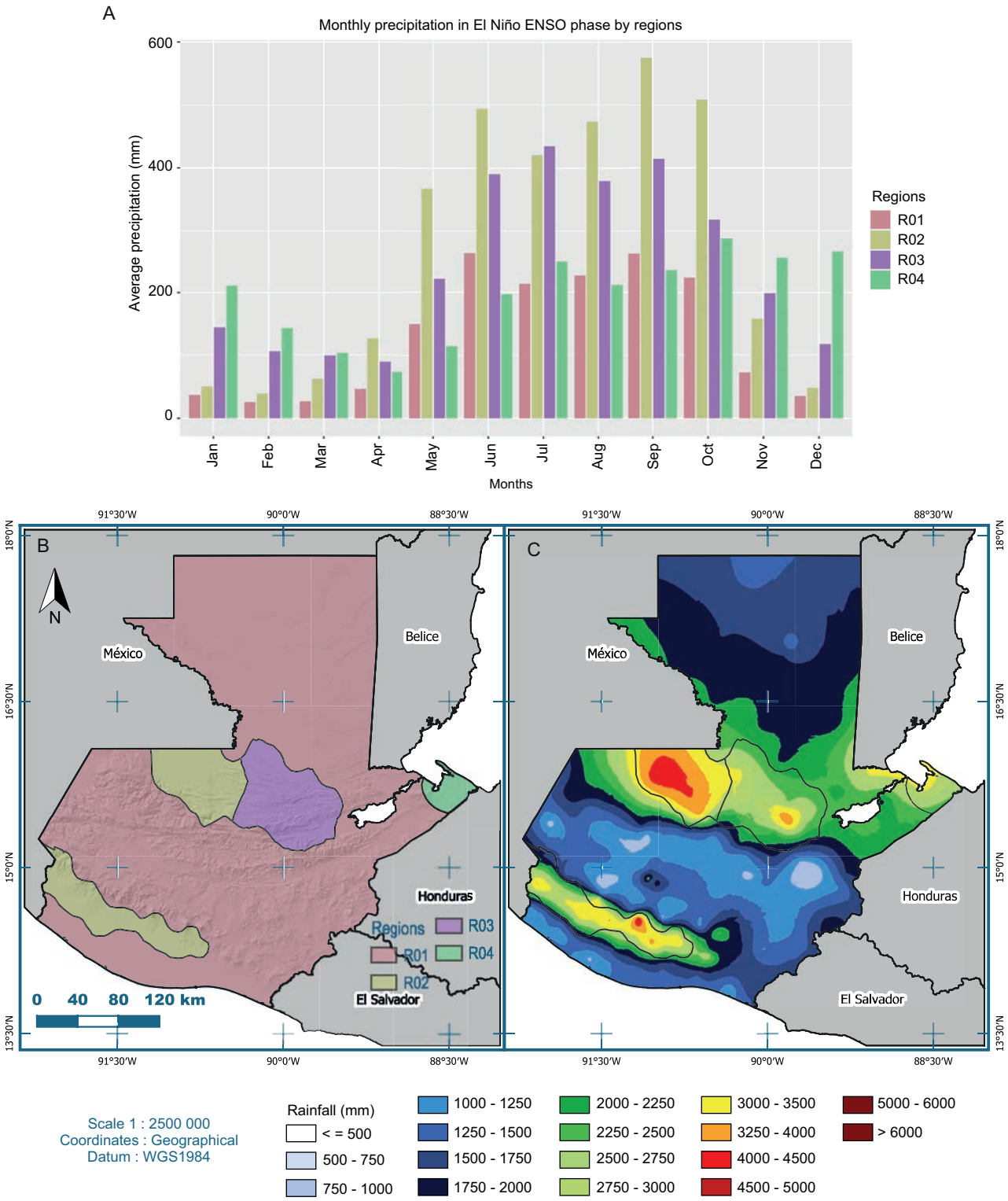

Figure S4. A. Regions and average monthly precipitation under El Niño conditions; B. El Niño conditions climate regions and its boundaries; C. Average annual precipitation under El Niño conditions and regions boundaries.